

Explaining Provenance-Based GNN Detectors with Graph Structural Features

Kunal Mukherjee, Joshua Wiedemeier, Tianhao Wang, Muhyun Kim, Feng Chen,
Murat Kantarcioglu, and Kangkook Jee

Department of Computer Science, The University of Texas at Dallas

Abstract

The opaqueness of ML-based security models hinders their broad adoption and consequently restricts the transparent security operations due to their limited verifiability and explainability. To enhance the explainability of ML-based security models, we introduce PROVEXPLAINER, a framework offering *security-aware* explanations by translating an ML model’s decision boundary onto the interpretable feature space of a surrogate DT. Our PROVEXPLAINER framework especially focuses on explaining security models that are built using GNNs since recent studies employ GNNs to comprehensively digest system provenance graphs for security critical tasks. PROVEXPLAINER uses graph structural features based on security domain knowledge gained from extensive data analysis, utilizing public and private system provenance datasets.

PROVEXPLAINER’s interpretable feature space can be directly mapped to the system provenance problem space, making the explanations human understandable. Because the security landscape is constantly changing, PROVEXPLAINER can be easily extended with new explanatory features as they are identified in the wild. By considering prominent GNN architectures (*e.g.*, GAT and GraphSAGE) for program classification and anomaly detection tasks, we show how PROVEXPLAINER synergizes with current SOTA GNN explainers to deliver domain-specific explanations. On malware and APT datasets, PROVEXPLAINER achieves up to 9.14% and 6.97% higher precision and recall, respectively, compared to SOTA GNN explainers. When combined *with* a general-purpose SOTA GNN explainer, PROVEXPLAINER shows a further improvement of 7.22% and 4.86% precision and recall over the best individual explainer.

1 Introduction

Given the significant threat posed by advanced and sophisticated adversaries [1]–[4], security is paramount in today’s highly digitalized society. Recent advances in pervasive monitoring, system event collection, and system provenance analysis have generated a variety of detailed telemetry for advanced

security analysis. To leverage this telemetry data to counter security threats, various learning-based security tools have been proposed and deployed [5]–[21]. Particularly, Endpoint Detection and Response (EDR) solutions [22]–[24], built on fine-grained system provenance data, have become a mainstream security defense for enterprise networks [25], [26]. System provenance captures causally dependent system events on an end host, represented as a provenance graph. Provenance graphs are heterogeneous (*i.e.*, different node and edge types with textual and numerical attributes) and efficiently represent subtle runtime behaviors. Hence, provenance graphs provide irreplaceable security defense for countering sophisticated and stealthy APT-like attack campaigns.

The rising popularity of provenance graphs has increased interest in leveraging Graph Neural Networks (GNNs). Recent advancements in GNNs provide framework-level support for directly learning relational dependencies and topological structures from graphs. GNNs employ a message-passing mechanism that aggregates information from adjacent nodes and edges, expanding the neighborhood with each additional layer. Automatically learning from complex graph datasets has proven beneficial across various domains. GNN-based security models are highly effective in leveraging system provenance graphs. However, the advantages are considerably diminished by the models’ opaque nature, specifically the absence of clear explanations for their predictions. These models do not provide explanations that are *security-aware*¹, which is essential for security practitioners to build trust.

Studies [27]–[29] have attempted to provide domain-agnostic explanations for GNN decisions, but they lack verification in the security domain, where contextualizing the explanations with program behaviors is critical in building trust in the underlying model. While recent works [30]–[32] have emphasized verifiable explanations for Neural Networks (NNs) in binary analysis and vulnerability discovery, *our study is the first to verify explanations in the system provenance domain.*

¹Within this framework, security-aware explanations refer to those grounded in the specialized techniques, threats, and requirements familiar to professionals in the security field.

In this paper, we propose a novel approach to enhance the trustworthiness of the decision-making process of complex GNN models built on system provenance data by equipping interpretable surrogate Decision Trees (DTs) with *security-aware graph structural features*. Via extensive data study, we develop features that capture several graph substructures that correspond to well-known malicious activities such as drive-by-download (*e.g.*, dropper malware) [33], [34], malware staging and propagation [35], system probing [36], and malware replication using templates [37]. These features facilitate interpretability by security experts [38] by closely capturing security-relevant system behaviors.

Our research effort decouples the feature engineering and decision-making of performance-critical models, with a focus on using feature engineering to assist *human interpretation* rather than improving decision accuracy. The core insight behind our study is that general purpose explanation techniques are missing security-specific considerations, but can be supplemented with security-specific structural features to close the gap. We stress that PROVEXPLAINER is an *explanation technique, not an attack detection technique*. Compared to GNNs, the surrogate DTs trade away generalizability, expressiveness, and automatic feature extraction to obtain interpretability, which makes them unsuited for attack detection. Although PROVEXPLAINER utilizes carefully crafted security-aware graph features, there is potential for incorporating additional features into our framework for enhanced explanations. Consequently, PROVEXPLAINER is designed to be easily extendable with other security-aware graph features.

While PROVEXPLAINER independently surpasses current State-Of-The-Art (SOTA) GNN explainers in the majority of our security-oriented evaluation tasks, as we show in our experimental evaluation, it can also be seamlessly integrated with other SOTA GNN explainers to develop even more effective explanations. Lastly, PROVEXPLAINER works only on graph structural features of the system provenance graphs. While we have a plethora of security analyses that work on numerical and textual labels and attributes, we believe that the core strength of graph-structured datasets lies in their structural features.

To demonstrate the advantages of PROVEXPLAINER in the system provenance domain, we compared PROVEXPLAINER against SOTA GNN explainers such as GNNExplainer [27], PGExplainer [28], and SubgraphX [29] across well-balanced security domain tasks, including program classification, malware detection, and Advanced Persistent Threat (APT) detection. These SOTA GNN explainers provide the best performance according to other security studies [31], [39]. The GNN models in our evaluation are trained with an extensive dataset collected using our in-house deployment which monitored system events on an average of 20 mixed Windows and Linux hosts over 13 months. In addition, in our evaluation, we used the DARPA [40] Transparent Computing dataset, the APT dataset from [41], and Fileless Malware lists from [42].

Table 1: Node and edge types for in-house system provenance with associated attributes.

| | Types | Attributes |
|----------------------|----------------------|--------------------------------------|
| Nodes (resources) | process | signature, executable name, pid |
| | file | owner (uid, gid), name, inode |
| | socket (IP) | dstip, srcip, dstport, srcport, type |
| Edges (events) | process → process | command args, starttime |
| | process → file | read, write, amount |
| | process → IP address | send, recv, amount |

To our knowledge, our research is the first to leverage security-aware graph structural features specifically tailored for human interpretation. Broadly, we summarize the contributions of PROVEXPLAINER as follows:

- PROVEXPLAINER examines graph structural features linked to system actions by conducting extensive data studies aided by security domain knowledge.
- Our security-aware features enabled surrogate DTs to achieve 88% agreement on APT and Fileless Malware detection and 83% agreement on program classification.
- We curated an extensive dataset using in-house data collection, APT datasets from different sources (*i.e.*, industry standard DARPA [40] and past literature [41]) and collected real-world Fileless malware samples from [42] to confirm the generalizability of PROVEXPLAINER.
- PROVEXPLAINER improves precision by 9.14% and recall by 6.97% compared to GNNExplainer [27], PGExplainer [28], and SubgraphX [29], which are the current SOTA GNN explainers.
- Combining PROVEXPLAINER with SOTA GNN explainers improves the precision and recall by 7.22% and 4.86% over the best individual explainer.

To benefit the community and facilitate future research, we are committed to publish our dataset and code.

2 Background and Related Work

We introduce system provenance and its learning-based security applications. We discuss the efforts made to explain GNN models and their challenges. Finally, we discuss the verification of explanations in the system provenance domain.

2.1 System Provenance and Data Collection

System provenance analysis [15], [43]–[45] leverages data collection agents on end-hosts to collect interaction events among key system resources: processes, files, and network sockets. This work relies on in-house data from 21 hosts in a university, the DARPA Transparent Computing dataset [40], and datasets from previous studies [41]. Our in-house data collection accumulates 13 GB to 92 GB daily, tracking around 875 unique programs, 7,025K processes, 4,824K network connections, and 111,583K file operations.

Our system provenance data schema, detailed in Table 1, is similar to DARPA’s research-oriented Common Data Model (CDM) [40] schema, but we omit memory objects, registry events, and thread distinctions within a process. These choices were made to balance real-world overhead constraints of load balancing and storage. We also established a malicious testbed to generate malware execution traces. To ensure the freshness and realism of our malware samples, we utilize Cyber Threat Intelligence (CTI) feeds [46], the VirusTotal API [47], and penetration testing tactics, techniques, and procedures (TTPs) [48]–[50]. We refer to [40] and [41] for APTs.

2.2 Provenance-based ML Security Solutions

Recent advancements in system event collection have revitalized host-based Intrusion Detection Systems (IDSs). Although initially proposed in the late ’90s [51], host-based IDSs have proved effective against advanced attacks such as APTs and Fileless Malware. Various studies [15], [18]–[21], [52], [53] demonstrate the efficacy of provenance-based Machine Learning (ML) techniques in identifying behavioral deviations. However, the high detection performance is offset by a lack of trustworthy explanations and high false positive rates, impacting operational confidence and resource allocation. Detection tasks are prone to errors and are difficult to verify without full knowledge of typical behaviors. Our work focuses on enhancing the transparency and explainability of provenance-based ML security. We concentrate on a balanced set of security tasks: Malware detection, APT detection, and program classification. In this paper, we consider graph-level tasks; providing explanations for node and edge level tasks is a promising direction for future work that aligns with upcoming security detection system trends.

GNNs for System Provenance. Our research employs an industry-standard GNN framework to model and explain system provenance graphs, leveraging DGL’s mature development ecosystem [54] for alignment with current analytical techniques and streamlined integration into real-world applications. Despite the security community’s historical preference for custom detectors² [19]–[21], [52], [53] due to the complexity and heterogeneity of provenance graphs, we chose a general GNN framework for long-term integration benefits and broader impact. Notably, the DGL community has integrated our heterogeneous GNN enhancement.

2.3 Explainability and Security Applications

Explaining ML Security Models. Due to the importance of explainability in the security domain, several explainers have been proposed for ML-based security analysis. LEMNA [55]

²It has only been recently that GNNs have started gaining attention within the community. Certain provenance-based ML detectors were even proposed before GNN frameworks became popular.

focused on classifying PDF malware and detecting a function’s entry point in binary code using regression mixture models as a localized surrogate to approximate the classifier’s decision boundary. Recent works such as CFGExplainer [56] and FCGAT [57] use deep surrogate models to explain GNN-based malware detection using control flow graphs or function call graphs. These methods exclusively work on homogeneous graphs, thus cannot be directly applied to provenance domain.

Jacob et al. [58] proposed TRUSTEE, a framework that generates DT-based interpretations for ML models to detect shortcut learning (*e.g.*, problem underspecification). Their success clarifying model decisions about network packets inspired us to generalize the approach to the system provenance domain. The core challenge is that the system provenance domain relies on highly heterogeneous graph datasets, which are not natively consumed by DTs. By leveraging security-oriented graph structural features and cooperating with general-purpose GNN explainers, PROVEXPLAINER enables DT-based explanations in the provenance domain.

Explaining GNN Models. Recent research in GNN explainers [27]–[29] has advanced in identifying key nodes, edges, or subgraphs in GNNs, and are categorized into white-box and black-box explainers. White-box methods, *e.g.*, GNNExplainer [27] and PGExplainer [28], access GNN internals, including model weights and gradients. Conversely, black-box methods like SubgraphX [29] operate on model inputs and outputs, reducing coupling between the explanation framework and model architecture.

2.4 Ground-truth Verification

In system provenance, “ground truth” refers to the real-world information against which the validity of a model’s predictions are checked. In this paper, we approximate the ground truth using documentation created by security vendors, tech reports, and previous studies. The relevant processes, files, and network sockets mentioned in the documentation are designated as *documented entities*. We understand that the documentation provided by the security vendors can have experimental errors, as well as selection and experimental bias. To mitigate these problems, we aggregated information from multiple security vendors.

We extract *documented entities* with three methods: (1) referring to pre-existing malware profile databases that contain information from different security vendors, such as VirusTotal [47], we obtain activity summaries detailing network communications, file system actions, and process behaviors; (2) we extract key entities (*i.e.*, process involved, files created and connections made) from tech reports [59], [60] and system manuals [61]; (3) we consult dataset authors [41] and review dataset documentation to identify the components of each attack present in the datasets.

Ground truth verification of ML model decisions in security-critical tasks has garnered significant attention, un-

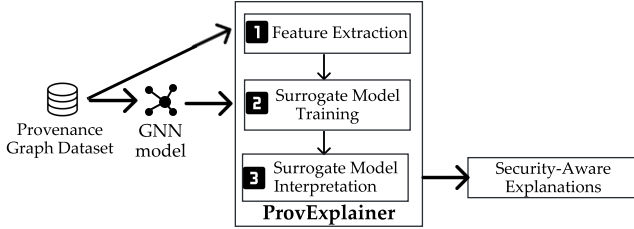


Figure 1: PROVEXPLAINER architecture.

derscoring the role of explanations in unveiling the truth [30]–[32]. These studies highlight the effectiveness of white-box techniques in malware detection and vulnerability discovery, with further advancements in reconstructing ground truth around local explanations [32]. [62] has shown high variance in explanations provided by traditional GNN explainers, raising reliability and applicability concerns.

3 Problem Statement and Threat Model

Our research addresses explainability in GNN security models built on system provenance graphs, tackling a core issue in the security domain. The complexity of explaining GNN decisions is exacerbated by graph structural learning, which adds to the inherent complexity of NNs. Existing studies on GNN explainability [27]–[29], [32], [56], [63] often fail to effectively map back to system behaviors in the provenance domain. To bridge this gap, our design approach aims to explain GNN decisions by employing a surrogate DT equipped with interpretable security-aware graph structural features.

Our threat model assumes the integrity of on-device data collection, relying on provenance records secured by existing systems ([15], [18]–[21], [41], [44], [45]). Our primary objective is to generate security-aware explanations to aid security practitioners and increase their trust in the GNN’s decisions. We consider graph-level classification and anomaly detection tasks; explaining GNN decisions in node/edge level tasks is outside the scope of this work. Systematically generating an accurate and trustworthy ground truth for application, malware, and APT behavior is a challenging open problem. In this paper, we approximate the ground truth using publically available documentation (§2.4). In line with recent literature on GNN explanation [30], [31], [56], adversarial samples are outside the scope of the paper. Creating robust detection and explanation systems that can withstand adversarial manipulation [41], [64], procedural dataset poisoning, and model manipulate are critical open research problems that are orthogonal to our work.

4 PROVEXPLAINER Overview

Given a GNN model built with a system provenance dataset, we apply PROVEXPLAINER in three stages, refer to Figure 1.

| APT | Attack Vector | Subgraph Structure |
|---------------------------------|---------------|----------------------------------|
| Initial Compromise § 4.1.1 | Staging | Dropper Triangle, Cascade |
| Establish Foothold § 4.1.2 | Cloning | Clone Triangle, Probe Triangle |
| Deepen Access § 4.1.3 | Inheriting | Kite, Jellyfish |
| | Sharing | Square |
| Lateral Movement § 4.1.4 | Accessing | Exploding Kite, Exploding Square |
| Look, Learn, and Remain § 4.1.5 | Exfiltrating | External IP Use |

Table 2: Summary of program behavior patterns.

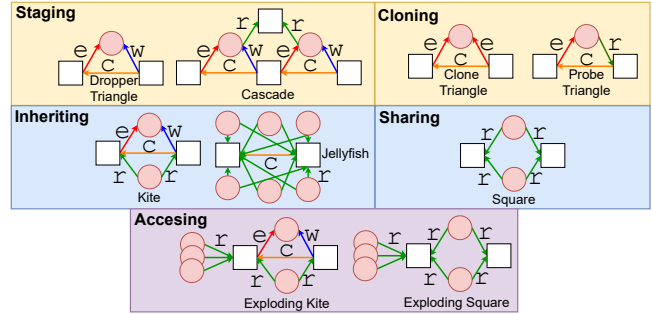


Figure 2: Structural Graph Features. Squares are processes and circles are files. Write edges are blue, read edges are green, execute edges are red, and process creation edges are orange.

Stage 1: Extract Security-aware Features (§4.1). Using a data-driven approach (Algorithm 1), we extract security-aware subgraphs (Table 2) that exhibit distinctions between benign and anomalous datasets (Figure 3). These subgraphs identify attack vectors used by APTs.

Stage 2: Train an Interpretable Surrogate Model (§4.2). Next, we utilize an extensive and diverse system provenance dataset (§A.1) to train an interpretable surrogate DT to agree with the GNN using the extracted features.

Stage 3: Interpret the Surrogate Model (§4.3). To extract the explanation for a detection using the surrogate DT, we designed Algorithm 2 to extract the graph nodes that contribute to the surrogate DT’s decision. These explanations are valid only when the surrogate agrees with the GNN.

4.1 Graph Structural Features

Subgraph patterns are the foundation of PROVEXPLAINER’s interpretable graph features. They are localized in the provenance graph and correspond to distinct program behaviors in computer systems. The security landscape is continuously evolving, with the MITRE ATT&CK framework documenting over 367 attack vectors [65], and new vectors being added regularly. To adapt to evolving threats [66] by automatically extracting structural features from data, we designed Algorithm 1 to systematically extract subgraph patterns that exhibit a distribution difference between classes within a dataset. We first generate all semantically valid subgraphs of a given size. For example, every edge must contain to at least one process node because only processes can take actions. We then count

Feature Distribution Across Datasets

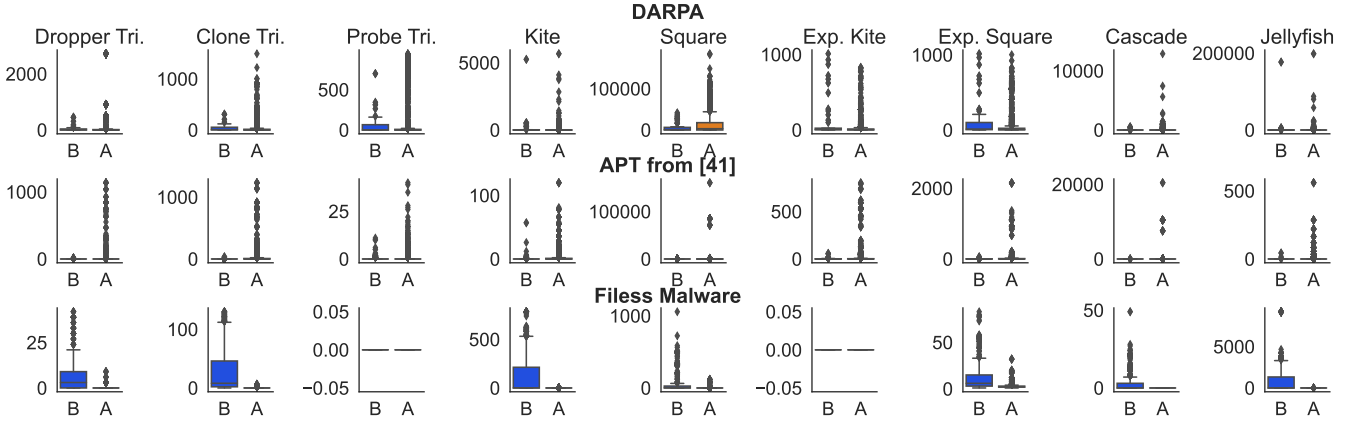


Figure 3: Distribution of nine subgraphs (Table 2) in different datasets. *B* means benign and *A* means anomaly.

the instances of each of these subgraphs for each class in the dataset. Finally, we sort the subgraphs by the magnitude of the distribution difference between the classes to obtain the most effective structural features.

However, subgraph pattern mining is resource intensive and scales exponentially in the size of the subgraphs; there are 56 semantically valid 3-node graphlets, and even adding just one more node increases that count to 887. Optimizing the identification and mining of subgraphs is a critical active research area [67]–[71]. After analyzing the 56 semantically valid 3-node graphlets and selecting the top 3 strongest contributors, we expedited the analysis of larger graphlets by applying domain expertise and data study to significantly reduce the search space. This way, we obtained 9 patterns that capture common attack vectors (Figure 2). We validated these patterns by measuring the distribution difference across data classes (Figure 3). Although the *Probe Triangle* and *Exploding Kite* patterns are not well-represented in the Fileless Malware dataset, their strong signals in the APT datasets justify their inclusion. Subgraph structures that map directly to attack vectors aid in generating security-aware explanations.

Algorithm 1 Graph Structural Feature Extraction

Require: Dataset D , Node size n
1: $subgraphs \leftarrow GetFeasibleSubgraphs(n)$
2: $count \leftarrow []$
3: **for** each $graph, label$ in D **do**
4: $subgraph_cnt \leftarrow \{sg : CountSubgraphs(graph, sg) \mid sg \in subgraphs\}$
5: $counts.append([subgraph_cnt, label])$
6: **end for**
7: Aggregate the $subgraph_cnt$ count per $label$
8: Calculate the $subgraph_cnt$ difference between the labels
9: **return** $subgraphs$ sorted by largest difference in count

4.1.1 Initial Compromise

Staging. A prevalent attack vector in conducting the initial compromise [72] as seen in DARPA attacks [59] is to

save the malicious logic in temporary locations (e.g., `\tmp\` or `C:\Users\AppData\Local\Temp`) and then execute it. These temporary locations are often whitelisted by defense mechanisms. The attacker then performs initial compromise by executing the payload. Fileless Malware also contains “dropper” behavior [33], [34]. The *Dropper Triangle* and the *Cascade* structures (Figure 2) capture the dropper behaviors.

4.1.2 Establishing a Foothold

Cloning. Attackers taking advantage of multiprocessing-based parallelism for redundancy and efficiency to replicate malware instances to overload the system’s defenses is emblematic of establishing a foothold [73]. In the *Clone Triangle*, a parent and child process both execute the same program. Clone triangles are also common in benign programs that use multiprocessing as part of their standard workflow, such as `sc.exe` and `explorer.exe`. In the *Probe Triangle*, The attacker first probes the payload and necessary library files by reading them to ensure their existence before executing the payload, which is common in cryptominers [74]. This avoids suspicious events (e.g., accessing nonexistent files) from occurring and triggering defenses. While probing and cloning alone are not sufficient to indicate malicious activity, they amplify the importance of other attack behaviors. The *Clone Triangle* and the *Probe Triangle* (Figure 2) efficiently identify the cloning attack vector.

4.1.3 Deepen Access

Inheriting. After gaining initial access and establishing a foothold, attackers scale up their operations to deepen access [75]. These attackers create multiple child processes that execute the same payload. Because the children inherit their objectives from the parent, these parent-child malware pairs read similar library files. Advanced malware writers [74] also

update the configuration inside the malware payload to keep track of the system state to maximize resource consumption (e.g., CPU cycles, RAM, and network bandwidth) without triggering usage alerts. The *Kite* and the *Jellyfish* shape (Figure 2) efficiently identify inheriting behavior.

Sharing. Malware such as Banking Trojans [35], [76] do not directly create malware that access the sensitive documents but rather they create multiple process chains where the last process in the chain does the malicious behavior. APTs also create such process chains to obscure the point of entry and spread throughout the system. In these attacks, processes with distant ancestral relations demonstrate operational similarities by reading the same library files. The *Square* (Figure 2) pattern efficiently identifies this resource sharing behavior.

4.1.4 Lateral Movement

Accessing. After deepening access, the attacker reads sensitive resources (e.g., cookies and credential files) to enable lateral movement [77] through the system. Capturing the attacker’s intermediate objectives reveals additional resources the defender must protect. For example, in one of DARPA Trace’s [59] APT scenarios, the attacker reads sensitive configuration and cookies from `/home/admin/.mozilla/firefox/`, and `/usr/local/firefox-xx/obj-x86_64-pc-linux-gnu/` to advance their attack. The *Exploding Kite* and *Exploding Square* shape (Figure 2) identifies the resource accessing behavior.

4.1.5 Look, Learn, and Remain

We differentiate network nodes based on whether their IP addresses are internal or external to the system’s network. This critical feature requires minimal engineering effort but holds high security importance, as network behavior is extremely hard to hide. DoS malware [78] and APT threat actors commonly exfiltrate [79] data to their external command and control server. This behavior leads to a network node with a destination IP that is external to the local network.

4.2 Extracting Decision Trees

To obtain explanations from our security-aware graph structural features, we use them to train a global surrogate DT. By training a DT to agree with the predictions of a GNN model, we can interpret the DT to gain insights about the GNN’s decision-making process. To achieve the best agreement results, we enhance traditional DT training with data augmentation that iteratively increases the weight of incorrectly classified samples [58].

We begin with a labelled set of graphs $D_G = (G, Y)$, which is used to train the GNN. GNN’s predictions on D_G are collected, yielding $GNN(D_G) = Y'$. To prepare the dataset for training the DT, we extract the graph structural features (§4.1) S and

associate them with the GNN’s predictions Y' to create a labelled feature dataset $D_F = (S, Y')$, which we split into train, validation, and testing sets to evaluate the surrogate DT.

Leveraging the methods of Jacobs et al. [58], we use two-layer iterative dataset augmentation to train a series of DT models. At each iteration of the inner loop, all misclassified samples are duplicated to increase their weight in the next iteration; from this series of models, we select the one with the highest agreement among the DTs. This process is repeated several times in the outer loop, then the surrogate model with the highest mean agreement among those high-agreement DTs is selected as the final surrogate model for explanation. This improves the *stability* of the explanations, but at the cost of some agreement on smaller datasets. Because the surrogate model is aggregated over several iterations, the final resulting model is less sensitive to small changes in the training set.

4.3 Interpreting GNN Model Detections

Algorithm 2 Explanation for graph G .

Require: graph G , decision tree DT , explanation size k , max depth D

- 1: **function** EXPLAINGRAPH(G, DT, k, D)
- 2: $node_rankings \leftarrow \{v : 0 | \forall v \in G.V\}$
- 3: $dp \leftarrow GetDecisionPath(DT, G)$
- 4: **for** depth $d = 1$ to D **do**
- 5: $shape \leftarrow$ shape corresponding to rule at depth d in dp
- 6: $importance \leftarrow \frac{1}{d}$
- 7: **for** each node $v \in G.V$ that participates in $shape$ **do**
- 8: $impact \leftarrow$ # instances of $shape$ that n participates in
- 9: $score \leftarrow importance \cdot impact$
- 10: $node_rankings[v] \leftarrow \max(node_rankings[v], score)$
- 11: **end for**
- 12: **end for**
- 13: **return** the top-scoring k nodes from $node_rankings$
- 14: **end function**

Once the surrogate DT is trained, not only can we qualitatively analyze the DT for global insights, but we can also use it to explain decisions about individual graphs. Similar to existing explainers, we will assign an importance score to each node in the graph, then return the most important nodes. Each decision node within the DT consists of a subgraph structure and a threshold. Decision nodes closest to the DT root have the greatest influence on the decision path. In our experiments, we empirically found that considering DT nodes up to a depth of $D = 4$ yielded the best explanations in our datasets; lower depths missed shapes that were necessary for some complex APT scenarios and higher depths incorporated irrelevant system behaviors.

The crux of this methodology lies in ranking the provenance graph nodes based on two pivotal criteria: the importance of the decision node within the decision tree (assigning more importance to nodes that are closer to the root) and the impact of the node on the rules, assessed by the node’s biggest contribution to the features used by the rules. Such an approach not only aids in pinpointing critical nodes but also in understanding their roles in the broader context of system interactions. System attributes (e.g., process/file names, and

socket IP/port) can be extracted as a post-processing step. Finally, we use the interpretable surrogate DT to construct actionable, security-aware explanations about individual decisions. Because PROVEXPLAINER yields a global surrogate DT, domain experts can analyze it to improve their understanding of the GNN’s decision-making process.

4.4 Combining Explanation Methods

Algorithm 3 Combined explanation for graph G .

Require: graph G , explanation size k , PROVEXPLAINER’s node ranking R_1 , general-purpose explainer’s node ranking R_2

```

1: function ENSEMBLEEXPLANATION( $G, k, R_1, R_2$ )
2:    $combined \leftarrow \emptyset$ 
3:   for  $i = 1$  to  $k$  do ▷ Explainers take turns picking new nodes
4:     if  $i$  is odd then
5:        $combined \leftarrow combined \cup \text{argmax}_{v \in G.V} (R_1(v) | v \notin combined)$ 
6:     else
7:        $combined \leftarrow combined \cup \text{argmax}_{v \in G.V} (R_2(v) | v \notin combined)$ 
8:     end if
9:   end for
10:  return  $combined$ 
11: end function

```

When explainers are viewing the GNN’s decisions from different angles, it is often beneficial to consider input from multiple explanations to create a combined view of the important elements of the graph. In Algorithm 3, we present a method for merging the top ranking nodes from multiple explainers’ perspectives. By going through the explainers in a round-robin fashion, we ensure that the top-ranking nodes from each explainer are fairly represented in the final result.

PROVEXPLAINER provides explanations that are guided towards security-relevant graph structures, while traditional GNN explainers focus entirely on structures that are important to the GNN model. Our evaluation (§5.5) and case studies (§6) will show that, although PROVEXPLAINER more consistently identifies documented entities than traditional GNN explainers, these methods often emphasize different attack chain components. Taking the most confidently indicated nodes from each explainer often results in better explanations than any one explainer can achieve independently.

4.5 Implementation

Our data collection module can operate on Windows systems by using the Windows ETW [80] and on Linux system by using Linux auditd [81] frameworks to collect relevant system calls regarding files, processes and network sockets. These include system calls for (1) file operations (e.g., `read()`, `write()`, `unlink()`), (3) network socket operations (e.g., `connect()`, `accept()`), (4) process operations (e.g., `create()`, `exec()`, and `exit()`). The system-level data is stored in a PostgreSQL database. Table 1 summarizes the event collection schema for our in-house deployment.

PROVEXPLAINER is implemented using python and graph generation framework is implemented in java. The GNN

training and evaluation pipelines are implemented using Deep Graph Library (DGL) [54] framework, and the surrogate DTs are implemented using sklearn [82].

5 Evaluation

In this section, we evaluate PROVEXPLAINER’s effectiveness in explaining stealthy attacks. We aim to answer the following research questions (RQs):

- RQ1: Explanation Accuracy.** Can PROVEXPLAINER explain APT and Fileless malware detection (§5.3, §5.4)?
- RQ2: Comparison with SOTA GNN Explainers.** How do the explanations of PROVEXPLAINER compare against those of SOTA GNN explainers (GNNE explainer [27], PGExplainer [28], and SubgraphX [29]) (§5.5)?
- RQ3: Explanation Ensemble.** Can PROVEXPLAINER’s explanations be combined with those of SOTA GNN explainers to improve explanation stability (§5.5)?

5.1 Evaluation Protocols

For APT detection, Fileless Malware detection, and program classification tasks, we leveraged three kinds of datasets: (1) publicly available APT attack simulations [40], [41], (2) execution traces of Fileless Malware [42], and (3) program execution traces collected from our in-house testbed. We implemented two general purpose SOTA GNN models: GAT [83] and GraphSAGE [84], following the approach of recent explanation literature [56], [62]. Recent GNN based anomaly detection systems [20], [53] rely on custom node and edge embeddings for security tasks, so we did not evaluate against these specialized solutions. We conducted an ablation study and evaluated the explanations given by PROVEXPLAINER against those of SOTA GNN explainers [27]–[29].

Evaluation Metrics. In our evaluation of PROVEXPLAINER, we focus on two critical aspects. The first is the agreement of the surrogate DTs with the GNN model, which we measure using the weighted macro averaged (WMA) F1 score of the surrogate DT’s predictions with respect to the GNN’s predictions. The *agreement* metric gauges the faithfulness of the DT in replicating the conclusions of GNNs. The choice of the WMA F1 score accounts for the data imbalance issue prevalent in the anomaly detection datasets.

To evaluate PROVEXPLAINER’s and SOTA GNN explainers’ proficiency in identifying security-relevant entities, we define precision and recall metrics with respect to documented entities §2.4. A graph explanation method EM will yield a total ordering over V for a given graph $G = (V, E)$ and graph model M . Let V_k be the top k nodes according to $EM(G, M)$. Let D be the set of documented entities. *Precision* is the proportion of explanation nodes that are documented, and *recall* is the fraction of documented entities retrieved: $precision(V_k, k, D) = \frac{|V_k \cap D|}{k}$, and $recall(V_k, D) = \frac{|V_k \cap D|}{|D|}$.

5.2 Evaluation Tasks

APT Detection. We utilized the DARPA Transparent Computing (TC) Data Releases [40] and previous literature [41] for APT attack detection. This dataset, encompassing various OSes, provides a comprehensive basis for advanced security research. The DARPA APTs were designed to attack a system which consists of long-running processes and captured the stealthy attack vectors frequently employed by advanced adversaries. We particularly focused on three DARPA datasets used by previous studies [19]–[21], [53]: FiveDirections, Trace, and Theia. However, these tasks were conducted in a simulated environment and lasted for two weeks, involving a limited number of hosts. Therefore, we also evaluated against the APT scenarios conducted by [41], which were performed with realistic benign background workloads.

Fileless Malware Detection. For Fileless Malware detection, we targeted a family of stealthy malware samples that impersonate benign programs, evading conventional security solutions but are detectable by GNN-based provenance analysis. The malware samples were chosen in accordance with guidelines from the literature [85], [86] to minimize experimental bias and ensure freshness. The Fileless Malware dataset includes various categories [85], including banking Trojans, ransomware, spyware, and malware installers, with detailed statistics presented in Table 6 in the appendix.

Program Classification. Our program classification task asks the GNN to distinguish between operational modes of versatile system programs whose runtime behaviors influenced by command line arguments. For example, we want to determine which `python` program is running between `certbot`, `update-apt-xapian-index`, `unattended-upgrade`, `decompyle3`, and `cuckoo`. We have similar datasets for `powershell.exe` and `firefox.exe`, which are described in detail in the appendix in Table 5. Our data collection, approved by the Institutional Review Board (IRB), involved system event data from volunteers’ Windows and Linux hosts, totaling 14 TB over 13 months. This data encompassed a variety of user workloads including students, researchers, developers, and administrators. The program classification task provides a reference point for this study because the classes are balanced, stabilizing the GNN’s decisions.

5.3 Graph Structural Feature Evaluation

To answer RQ1, Table 3 demonstrates the effectiveness of surrogate DTs in mirroring the decision process of GNN models like GAT and GraphSAGE. Agreement between the surrogate DT and the GNN is an important metric for two reasons: (1) surrogate explanations are only valid when the surrogate agrees with the GNN, and (2) high agreement indicates that the surrogate model is a good approximation of the GNN’s decision-making process.

The APT datasets exhibit high agreement (> 87%) with

Table 3: Surrogate DTs have high agreement with the decisions of GNN measured using the WMA F1 score. Grey cells low agreement with the GNN (discussed in §5.3).

| Dataset | GAT | Surrogate DT (agree w/ GAT) | GraphSAGE | Surrogate DT (agree w/ GraphSAGE) |
|-----------------------------|------|--------------------------------|-----------|--------------------------------------|
| APT Dataset from [41] | | | | |
| Enterprise | 0.97 | 0.93 | 0.94 | 0.92 |
| Supply-Chain | 0.87 | 0.90 | 0.84 | 0.91 |
| Average | 0.91 | 0.92 | 0.89 | 0.92 |
| DARPA APT Dataset [40] | | | | |
| FiveDirections | 0.72 | 0.88 | 0.69 | 0.87 |
| Trace | 0.67 | 0.90 | 0.65 | 0.92 |
| Theia | 0.69 | 0.90 | 0.59 | 0.90 |
| Average | 0.69 | 0.89 | 0.64 | 0.90 |
| Fileless Malware from [42] | | | | |
| <code>explorer.exe</code> | 0.99 | 0.79 | 0.95 | 0.67 |
| <code>wmic.exe</code> | 0.89 | 0.66 | 0.87 | 0.89 |
| <code>reg.exe</code> | 0.94 | 0.96 | 0.90 | 0.93 |
| <code>sc.exe</code> | 0.99 | 0.99 | 0.93 | 0.63 |
| <code>python.exe</code> | 0.97 | 0.79 | 0.95 | 0.75 |
| <code>svchost.exe</code> | 0.99 | 0.84 | 0.99 | 0.81 |
| Average | 0.96 | 0.83 | 0.88 | 0.83 |
| Program Classification | | | | |
| <code>python</code> | 0.90 | 0.85 | 0.77 | 0.71 |
| <code>powershell.exe</code> | 0.92 | 0.97 | 0.87 | 0.97 |
| <code>firefox.exe</code> | 0.83 | 0.80 | 0.65 | 0.70 |
| Average | 0.88 | 0.87 | 0.76 | 0.79 |

the GNN models, but the Fileless Malware and classification datasets only showed moderate agreement (> 79%). The graph structural features were designed with APT structures in mind, and are optimized to capture malicious behavior. The surrogate DTs’ superior performance in APT datasets can be attributed to PROVEXPLAINER’s optimized graph shapes that effectively capture the behaviors of the APT stages. Focusing on the `python` and `firefox.exe` classification datasets, where GraphSAGE performed relatively poorly, the surrogate DTs were unable to closely approximate the GraphSAGE model using the graph structural features. For example, `firefox.exe` creates *Jellyfish* shapes both when users browse for content and when system programs use it to download updates, since in both instances `firefox.exe` creates a child that reads the same system files (e.g., `System32`). The ablation study, Table 4 shows that the *Jellyfish* shape performs the worst for `firefox.exe`.

In the Fileless Malware datasets, two distinct scenarios emerge. First, in `explorer.exe` and `python.exe`, the surrogate DTs show poor agreement with both the GAT and GraphSAGE models. These datasets are dominated by malware using stealthy techniques such as *living-off-the-land*, which involve memory object interactions which are currently not captured in our provenance graphs. The absence of the distinguishing features impairs the effectiveness of PROVEXPLAINER. Secondly, there are cases where the surrogate DT’s agreement is poor with only GAT (`wmic.exe`) or only GraphSAGE (`sc.exe`). This variation arises because PROVEXPLAINER’s data augmentation methods aim to enhance stability at the expense of agreement. Consequently, in datasets with very few anomalous examples, like those of `wmic.exe`

and `sc.exe` (Table 6), the surrogate DTs’ performance becomes unstable which is an inherent limitation of the surrogate model approach [58].

PROVEXPLAINER’s graph structural features enable surrogate DTs to approximate GNN models’ decision-making process on in-distribution data. Although the features are sensitive to the data distribution, additional features can be extracted to extend support to new distributions.

5.4 Ablation Study

Table 4 shows the contributions of each structural feature to the overall agreement of surrogate DTs approximating a GAT model. We take the number of nodes and edges in the graph as a simple baseline, which obtains an average F1 score of 0.63 across our datasets, demonstrating that graph size alone is insufficient. Attack subgraphs typically represent a small portion of an overall provenance graph, so the graph size is an unreliable way to determine if an attack is present in the graph. Interested readers may find this study with GraphSAGE in the appendix, Table 8.

Security Domain Features. *Triangles* are tight parent-child process interactions, which are crucial in Fileless malware scenarios where a malware is creating the initial infection by dropping and cloning its payload to create multiple copies of itself. However, their simplicity also results in their prevalence in benign programs. In the DARPA datasets, long-running processes created similar amounts of triangles as the attacks. Therefore, it was difficult to reliably differentiate attacks from benign behavior, resulting in agreement with the GAT model being as low as 0.51. Some attacks, such as the `svchost.exe` Fileless malware samples, were frequently identifiable with triangles alone, since the benign program did not create triangles. Empirically, we have seen triangles are commonly a supporting feature that works alongside the more complex structures (e.g., *Exploding Square* and *Jellyfish*).

Squares and Kites form a reliable backbone for explaining anomaly detection and program classification decisions made by the GAT model. Boasting both the highest overall average agreement and top individual performances in the program classification and Fileless Malware detection tasks, squares and kites identify clusters of programs with shared dependencies. The *Kite* pattern is particularly effective at capturing malware replication and deployment because it contains a *Dropper Triangle* as a subgraph, but with the added requirement that the parent and child process share a dependency.

Exploding shapes are specializations of the *Square* and *Kite* patterns that include multiple file read operations by the child malware, and are therefore particularly effective at explaining the GAT’s predictions in the APT dataset from [41]. These exploding variants are created after the initial deployment, when the final payload is successfully executed. Consequently, the exploding shapes underperform in the benign program classification task as these are usually seen in equal quantity

in the benign context. It is noteworthy that exploding shapes perform very similarly to squares and kites.

Cascade and Jellyfish are used for identifying complex, multi-stage attacks. The archetypical *Cascade* pattern is a sequence of malware payloads with a central process monitoring its progress. The *Jellyfish* pattern simply identifies parent-child processes with many shared dependencies, which is common in parallel processing. These patterns are specialized towards process inheriting and staging behavioral scenarios, resulting in their excellent explanative power on the DARPA dataset, but showing high variability in their effectiveness for Fileless malware samples. This is because these shapes are prevalent in benign service applications (e.g., `sc.exe` and `explorer.exe`) since they are specialized for parallel processing and comprised of multiple child processes that attend to a service request. Therefore, this shape is prevalent in both benign and anomaly samples, resulting in a significant drop in explanative power compared to using the full feature list.

Internal and external network connections shows varying agreement depending on the attack scenario. For instance, in APT, network connections alone are not reliable indicators, as attackers often disguise their activities as legitimate programs that also establish network connections. However, attacks using programs that rarely make network connections, e.g., `reg.exe` or `sc.exe`, become easily identifiable.

All security domain features utilizing the full range of features generally results in the best overall performance. However, there are cases where a subset of features can perform almost as effectively as the complete set. This is evident in the case of `svchost.exe`, where the use of triangles alone achieves an agreement of 0.84, equal to that obtained with all features. This indicates the possibility of optimized feature selection in certain scenarios. Nevertheless, such optimization requires knowledge of the specific attack.

5.5 PROVEXPLAINER vs. SOTA Explainers

To answer RQ2 and RQ3, Figure 4 compares the precision and recall of explanations derived from SOTA methods (GNExplainer, PGExplainer, and SubgraphX) with those derived from PROVEXPLAINER. Generally, as we request more nodes from the explanation techniques, the precision trends downwards and the recall trends upwards. PROVEXPLAINER surpasses all existing SOTA explainers across datasets, barring the APT dataset mentioned in [41] for explanations exceeding 40 nodes. This exception arises due to PROVEXPLAINER’s capture of systemic noise for large window sizes, which impacts precision. Nonetheless, for the APT dataset in [41], PROVEXPLAINER excels in generating concise explanations below 40 nodes, aligning with the preferences of security researchers for brief yet comprehensive analyses. Later, we will analyze specific case studies in §6.

In the DARPA and APT datasets, the security-aware features of PROVEXPLAINER provide a clear advantage in ex-

Table 4: Agreement of surrogate DTs with the GAT model across different feature subsets. The best feature subsets are highlighted.

| Dataset | Number of nodes and edges | Security Domain Features §4.1 | | | | | All Security Domain Features |
|----------------------------|---------------------------|-------------------------------|---------------------|---------------------|-----------------------|--------------------------|------------------------------|
| | | Triangles | Squares and Kites | Exploding Shapes | Cascade and Jellyfish | Internal vs External IPs | |
| DARPA APT Dataset [40] | | | | | | | |
| FiveDirections | 0.58 (-0.30) | 0.51 (-0.37) | 0.85 (-0.03) | 0.85 (-0.03) | 0.84 (-0.04) | 0.79 (-0.09) | 0.88 |
| Trace | 0.61 (-0.29) | 0.60 (-0.30) | 0.84 (-0.06) | 0.84 (-0.06) | 0.88 (-0.02) | 0.79 (-0.11) | 0.90 |
| Theia | 0.68 (-0.22) | 0.75 (-0.15) | 0.86 (-0.04) | 0.84 (-0.06) | 0.88 (-0.02) | 0.82 (-0.08) | 0.90 |
| Average | 0.62 (-0.27) | 0.62 (-0.27) | 0.85 (-0.04) | 0.84 (-0.05) | 0.87 (-0.03) | 0.80 (-0.09) | 0.89 |
| APT Dataset from [41] | | | | | | | |
| Enterprise | 0.72 (-0.21) | 0.78 (-0.15) | 0.83 (-0.10) | 0.91 (-0.02) | 0.66 (-0.27) | 0.88 (-0.05) | 0.93 |
| Supply-Chain | 0.75 (-0.15) | 0.70 (-0.20) | 0.87 (-0.03) | 0.83 (-0.07) | 0.63 (-0.27) | 0.67 (-0.23) | 0.90 |
| Average | 0.73 (-0.18) | 0.74 (-0.18) | 0.85 (-0.07) | 0.87 (-0.05) | 0.65 (-0.27) | 0.78 (-0.14) | 0.92 |
| Fileless Malware from [42] | | | | | | | |
| explorer.exe | 0.57 (-0.22) | 0.76 (-0.03) | 0.77 (-0.02) | 0.77 (-0.02) | 0.46 (-0.33) | 0.69 (-0.10) | 0.79 |
| wmic.exe | 0.49 (-0.17) | 0.51 (-0.15) | 0.55 (-0.11) | 0.57 (-0.09) | 0.62 (-0.04) | 0.55 (-0.11) | 0.66 |
| reg.exe | 0.87 (-0.09) | 0.88 (-0.08) | 0.91 (-0.05) | 0.85 (-0.11) | 0.88 (-0.08) | 0.92 (-0.04) | 0.96 |
| sc.exe | 0.49 (-0.50) | 0.80 (-0.19) | 0.97 (-0.02) | 0.94 (-0.05) | 0.80 (-0.19) | 0.84 (-0.15) | 0.99 |
| python.exe | 0.71 (-0.08) | 0.78 (-0.01) | 0.79 (0.00) | 0.77 (-0.02) | 0.74 (-0.05) | 0.76 (-0.03) | 0.79 |
| svchost.exe | 0.74 (-0.10) | 0.84 (0.00) | 0.83 (-0.01) | 0.83 (-0.01) | 0.82 (-0.02) | 0.81 (-0.03) | 0.84 |
| Average | 0.65 (-0.19) | 0.76 (-0.08) | 0.80 (-0.04) | 0.79 (-0.05) | 0.72 (-0.12) | 0.76 (-0.08) | 0.84 |
| Program Classification | | | | | | | |
| python | 0.53 (-0.32) | 0.77 (-0.08) | 0.83 (-0.02) | 0.75 (-0.10) | 0.79 (-0.06) | 0.82 (-0.03) | 0.85 |
| powershell.exe | 0.63 (-0.34) | 0.81 (-0.16) | 0.75 (-0.22) | 0.82 (-0.15) | 0.65 (-0.32) | 0.95 (-0.02) | 0.97 |
| firefox.exe | 0.35 (-0.45) | 0.38 (-0.42) | 0.41 (-0.39) | 0.44 (-0.36) | 0.46 (-0.34) | 0.61 (-0.19) | 0.80 |
| Average | 0.53 (-0.34) | 0.77 (-0.10) | 0.83 (-0.04) | 0.79 (-0.08) | 0.82 (-0.05) | 0.75 (-0.12) | 0.87 |

Precision and Recall of Different Graph Neural Network Explainers

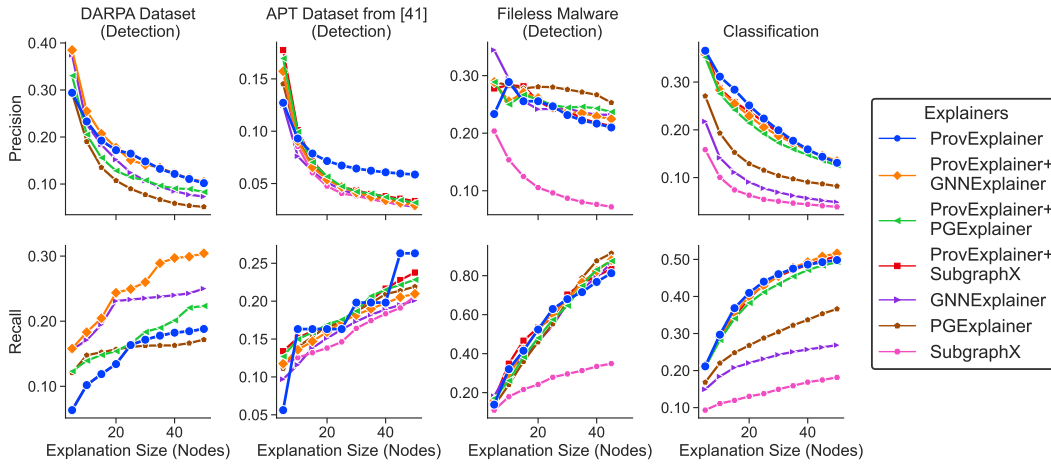


Figure 4: Effectiveness of graph model explainers at identifying documented entities (§5.1), measured using precision and recall.

tracting security-relevant nodes from the provenance graphs. In the APT dataset, we notice a limitation of PROVEXPLAINER, where it can only offer nodes that participate in the defined shapes for the explanation, which can lead to plateaus when there are security-relevant nodes that do not participate in any of the shapes. In the Fileless malware dataset, where the usage of memory objects disrupts several structural patterns, PROVEXPLAINER still provides the best explanations with respect to the documented entities.

Our experimentation showcased an interesting trend among the SOTA explainers: no one SOTA explainer consistently

outperformed the rest. GNNExplainer tries to identify substructures that provide maximum mutual information, while PGExplainer generates a probabilistic global model to explain the predictions. The differences in explanation performance across datasets gives insight regarding the data composition depending on if it is easier to create global explanations or local explanations. For the DARPA datasets it is hard to create generalized explanations since the DARPA dataset consists of different APT scenarios that are executed using different payloads and attack tactics. But for the APT dataset from [41], which consists of only two different APT scenarios, it is

easier to create global explanations, favoring PGExplainer.

More interesting trends emerge when we *combine* explanations (§4.4). Selecting nodes for the explanation according to both PROVEXPLAINER and a general-purpose explainer achieves best or near-best performance with respect to the documented entities across all of our datasets. Particularly in the program classification and fileless malware detection datasets, even when there is a large gap between two general-purpose explainers, combining them with PROVEXPLAINER improves and stabilizes the performance. As we will further explore in our case studies (§6), the different explanation techniques prioritize different aspects of program behavior, causing the composite explanations to be more complete and stable than individual explanations.

6 Case Studies

To demonstrate PROVEXPLAINER in a realistic setting, we analyze three case studies from the DARPA [40] datasets. In each study, we use an explanation size of 40 nodes and refer to the GAT model. We list the most important features from the surrogate DT and qualitatively analyze the explanations from PROVEXPLAINER and the SOTA GNN explainers. Detailed system-level analyses can be found in the appendix (§A.4).

6.1 FiveDirections: Browser Extension

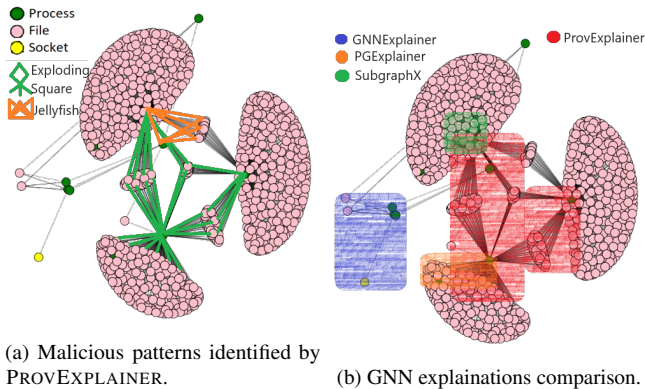


Figure 5: FiveDirections: the attacker exploits the target via a malicious Firefox extension.

Description. An attacker targets the Firefox browser using a malicious extension to deploy the drakon malware. The attacker writes drakon directly to disk and exploits a compromised browser extension masquerading as a password manager to execute malicious powershell code, gaining deeper access and control over the system, as illustrated in Figure 5a.

Features: *Exploding Square* and *Jellyfish*.

System Interpretation. This attack graph contains the *Jellyfish* and *Exploding Square* patterns, which are often observed

in the APT stages of *deepen access* [75] and *lateral movement* [77]. The *Jellyfish* pattern captures the dependency correlation among malware processes, where multiple instances of drakon exploit Firefox vulnerabilities via a malicious extension to spread to different parts of the system. This pattern is emblematic of malware processes cloning themselves to persist in the system as well as maintain operational integrity. Further, the *Exploding Square* highlights how malware processes move laterally to successfully exfiltrate sensitive data and read configuration files.

PROVEXPLAINER vs. SOTA explainers. Figure 5b compares the explanations of PROVEXPLAINER and those of SOTA GNN explainers, focusing on their efficacy in identifying security-aware elements. PROVEXPLAINER excels by highlighting the malware replicating itself from template files and accessing sensitive system files. PROVEXPLAINER isolates security-relevant structures in the graph, significantly increasing the end-user trust in the detection.

GNNExplainer identifies the malware template file and the malicious extension. This effectiveness stems from GNNExplainer’s method of searching for important edges. When this GNNExplainer isolates the pivot structure, the graph becomes disjoint, leading to a change in prediction. This results in a high information gain, the core metric for GNNExplainer. On the other hand, PGExplainer and SubgraphX reveal commonalities across attack graphs, such as the identification of key system library accesses required for malware operation. SubgraphX’s effectiveness varies due to its Monte Carlo Tree Search (MCTS), suggesting benefits to incorporating domain-specific insights into SubgraphX’s scoring function.

6.2 FiveDirections: Copykatz

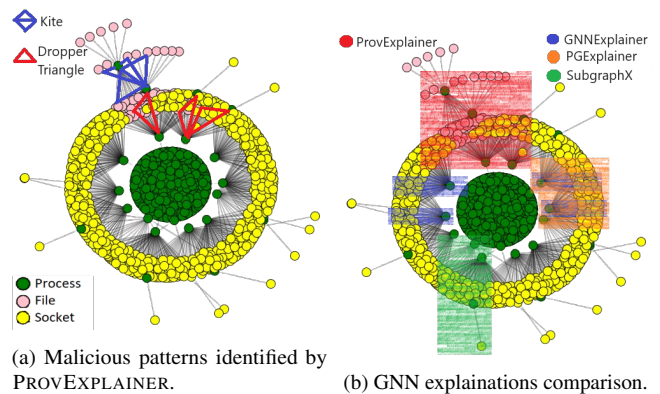


Figure 6: FiveDirections: the attacker gains C2 connections and installs Copykatz through a Firefox exploit.

Description. In a sophisticated attack, a hijacked version of `usdoj.gov` exploits Firefox to deploy drakon malware to the victim host. Then, drakon uses the *elevate* driver to escalate privileges and masquerade as the `runtimebroker` system

program. Finally, the malicious `runtimebroker` instance connects to a command and control (C2) server to download and execute `Copykatz` (an older version of `Mimikatz`) to harvest and exfiltrate host credentials.

Features: *Dropper Triangle* and *Kite*.

System Interpretation. The attack graph shown in Figure 6a highlights two key patterns: the *Dropper Triangle* and the *Kite*. The *Dropper Triangle* captures the initial access by highlighting the creation of malicious dynamic-link libraries. This stage enables the Windows Application Programming Interface and cryptographic operations necessary for the malware’s functionality. Following this, the malware disguises itself as `Firefox`, and executes the `Copykatz` payload.

The malicious `Firefox` instance then distributes its payload through temporary files, setting the stage for a subsequent malicious `Firefox` instance to trigger a flood of process creations. This chain of actions, marked by inherited functionalities from `Copykatz`, forms the *Kite* pattern. The replication of this malware leverages the same essential system libraries, indicating a meticulous design to maintain operational consistency throughout the malicious process chain.

PROVEXPLAINER vs. SOTA explainers. `GNNExplainer` and `PGExplainer` pinpoint the stage where multiple `Firefox` processes connect to the C2 servers. This activity traces back to the malicious `runtimebroker` instance. Notably, `SubgraphX` detects an alternate trajectory where a `Firefox` process, instead of reaching out to external servers, spawns another process aimed at local content manipulation, showcasing the malware’s versatility in engaging with both external and internal resources for its objectives.

While SOTA explainers have demonstrated proficiency in identifying the final stages of this data breach, only `PROVEXPLAINER` effectively captured both the initial infection and its propagation. This distinction underscores the importance of recognizing early-stage indicators for root cause analysis.

6.3 Trace: Phishing E-mail

Description. The attacker first launches a phishing campaign to compromise the identity of an employee. Leveraging the employee’s identity, the attacker then targets other employees with deceptive emails containing links to a malicious website. This website installs a Trojan in the victims’ computers, which then creates multiple copies of itself, overflowing the system. These cloned Trojans read sensitive user files while the original Trojan achieves persistence in the system.

Features: *Probe Triangle*, *Exploding Square*, and *Jellyfish*.

System Interpretation. In the Trace APT scenario, the *Probe Triangle*, *Exploding Square*, and *Jellyfish* patterns elucidate the malware’s structure (Figure 7a). The *Probe Triangle* reveals the Trojan’s cloning activity, where it is downloaded and replicates itself to establish a foothold. By masquerading as benign programs, the malware disguises its malicious

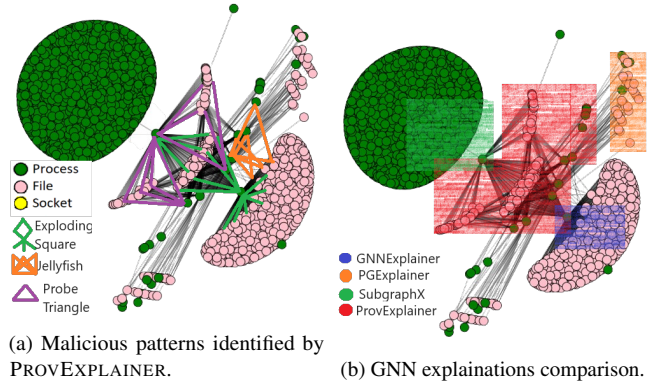


Figure 7: Trace: after an employee clicks on a phishing link, `Firefox` installs multiple Trojans to exfiltrate sensitive data.

processes, allowing it to proliferate undetected.

The Trojan, after establishing itself, impersonates system processes to execute a malicious script, leading to the creation of multiple copies. The *Jellyfish* pattern illustrates the dependency correlation among the cloned malware instances, interacting with similar system configuration files to operate efficiently as well as constructing a detailed profile of the target system. Ultimately, the extraction of data from sensitive system files is captured by the *Exploding Square*. This extraction is part of a larger scheme of lateral movement by profiling the available system processes, enabling the malware to leverage system libraries effectively.

PROVEXPLAINER vs. SOTA explainers. `GNNExplainer` identifies the initial malware staging behaviors, including interactions with shared libraries and cache files. Meanwhile, `PGExplainer` captures the benign structure of `xfce4-appfinder`—a lightweight desktop environment for UNIX systems, invoked by a DARPA script to simulate an enterprise environment. `SubgraphX` identifies the malicious inheritance behavior of `Firefox` executing a template to generate multiple malware clones. However, it overlooks sensitive file accesses, a detail exclusively captured by `PROVEXPLAINER`. `PROVEXPLAINER` comprehensively traced the malware kill chain from payload deployment and clone creation to the final step of accessing sensitive files.

7 Discussion and Future Work

GNN Model Capacity. *If decision trees trained with interpretable features provide accuracy comparable to GNN models, why do we need resource intensive GNN-based IDS?* In an IDS context, the automatic adaptability and generality provided by GNN models are necessary for quickly understanding the execution profiles of a wide variety of programs. DTs have many properties that, while unproblematic in an explanation setting, are highly undesirable for security detectors. Beyond the difference in expressive power, DTs require

labelled data, which can be provided by the GNN in an explanation setting, but will not be available for security detection. Further, DTs rely on features that are derived from known data and domain knowledge, so they are less able to generalize to unseen data. Therefore, for accurate and robust security detection, GNN models are strongly preferred.

Is PROVEXPLAINER Model Agnostic? PROVEXPLAINER is model agnostic and works on black-box provenance-based IDS. This line of research is not novel, as previous works [58], have used decision trees as surrogate models for deep neural networks before. PROVEXPLAINER’s novelty stems from the development of interpretable graph features to enable surrogate DTs to provide explanations for decisions about heterogeneous graph data in the system provenance domain. The interpretation of advanced graph features in the system provenance domain enables domain experts to better understand the system-level evidence used by provenance-based IDS.

Adversarial Manipulation of Graph Features. *What are the implications of attackers using knowledge of the graph structural features to design adversarial attacks against the explainer?* The explainer models used in PROVEXPLAINER is separate from the black-box detection model. Fooling both the interpretable surrogates and the underlying black-box model is the ideal case for an attacker seeking to avoid suspicion, and an attacker who can attack the explainer this way can also attack the detection model directly [41], [64]. Creating robust detection and explanation systems that can withstand adversarial manipulation is a critical open research problem, and is beyond the scope of this work.

Reliable Explanation for Unreliable GNN Models. Recent studies have made significant strides in investigating evasive attack generation against provenance-based ML detectors [41], [64], a noteworthy perspective that raises questions about the robustness and stability of the ML models in question. However, the core underlying assumption driving model explainer research — that the stability and trustworthiness of ML models can always be assured — may not necessarily hold. In future work, we plan to investigate the efficacy of model explainers under adversarial conditions in ML models could enhance their reliability, providing insights into their performance in real-world adversarial scenarios and contribute to the development of robust systems.

Behavioral Query Language for System Provenance. In the future work we hope to develop a graph query language using defined behavioral features to support efficient retrieval of provenance records based on program behaviors. The graph query will be based on the graph features, allowing the operator to search for programs using high level descriptions of their behavior, which will be converted into graph features in the query engine. The direction will also benefit significantly from advancements in subgraph mining algorithms. Future works may consider specialized provenance storage systems to optimize data retrieval.

Extending PROVEXPLAINER’s Feature Set. The security landscape is constantly evolving and no one dataset can provide a complete view of trending motifs in malicious behavior, so PROVEXPLAINER’s feature set will need to be periodically extended. Future work aiming to streamline this process by adapting advances in graph pattern mining [67]–[71] should note that interpretable features should be closely tied to local graph structures. Abstract features, like whole-graph eigenvector centrality, are difficult to attribute to individual nodes, and are therefore ineffective choices for interpretable features despite the potential for increased agreement with the GNN.

Support for Fine-Grained Detection Tasks. Recent developments in provenance-based security detection systems have trended towards fine-grained node and edge level anomaly detection [20], [53]. The explanation requirements of these detectors differ from those of whole-graph anomaly detectors and classifiers. In contrast to using explanations to narrow down the context for consideration by security practitioners, fine-grained models will need explainers to bring in relevant context to aid human analysis. Providing security-aware explanation support to advanced fine-grained security detectors is an exciting and important direction for future work.

8 Conclusion

We introduced PROVEXPLAINER, a framework that defines security-aware graph structural features and their corresponding system-level interpretations to address the pressing need for increased transparency and accountability in provenance-based IDS. Assisted with these features, simple interpretable DT models approximated GNN decisions on APT detection, Fileless Malware detection, and program classification tasks.

With extensive case-studies using real-world APTs, we confirmed that PROVEXPLAINER can assist in evaluating black-box detection models’ decisions in terms of interpretable security-aware graph structural features. We showed that explanations provided by PROVEXPLAINER improve precision and recall by 9.14% and 6.97% over SOTA GNN explainers with respect to attack documentation prepared by security vendors and dataset authors. Further, we successfully combined explanations from multiple explainers and demonstrated that the composite explanations are more stable and complete than their individual counterparts, resulting in an additional increase of 7.22% and 4.86% precision and recall over the best individual explainer.

References

- [1] A. Saini and H. Jazi, *North korea’s lazarus apt leverages windows update client, github in latest campaign*, <https://tinyurl.com/mr4h7d35>, Accessed: April 6, 2023, 2022.

- [2] D. Legezo, *Wildpressure targets industrial in the middle east*, <https://tinyurl.com/mr2n8hdu>, Accessed: April 6, 2023, 2019.
- [3] D. E. Sanger and N. Perloth, *U.s. said to find north korea ordered cyberattack on sony*, <https://tinyurl.com/5da2h9bx>, Accessed: April 6, 2023, 2014.
- [4] *Evasive attacker leverages solarwinds supply chain compromises with sunburst backdoor*, <https://tinyurl.com/bdz8s5yn>, Accessed: April 6, 2023, 2020.
- [5] G. E. Dahl, J. W. Stokes, L. Deng, and D. Yu, "Large-scale malware classification using random projections and neural networks," in *2013 IEEE International Conference on Acoustics, Speech and Signal Processing*, IEEE, 2013.
- [6] D. Arp, M. Spreitzenbarth, M. Hubner, H. Gascon, K. Rieck, and C. Siemens, "Drebin: Effective and explainable detection of android malware in your pocket.," in *Network and Distributed System Security Symposium (Ndss)*, Feb. 2014.
- [7] E. Gandotra, D. Bansal, and S. Sofat, "Malware analysis and classification: A survey," *Journal of Information Security*, 2014.
- [8] J. Saxe and K. Berlin, "Deep neural network based malware detection using two dimensional binary program features," in *2015 10th international conference on malicious and unwanted software (MALWARE)*, IEEE, 2015.
- [9] K. Grosse, N. Papernot, P. Manoharan, M. Backes, and P. McDaniel, "Adversarial perturbations against deep neural networks for malware classification," *arXiv preprint arXiv:1606.04435*, 2016.
- [10] B. N. Narayanan, O. Djaneje-Boundjou, and T. M. Kebede, "Performance analysis of machine learning and pattern recognition algorithms for malware classification," in *2016 IEEE National Aerospace and Electronics Conference (NAECON) and Ohio Innovation Summit (OIS)*, IEEE, 2016.
- [11] B. Kolosnjaji, A. Zarras, G. Webster, and C. Eckert, "Deep learning for classification of malware system call sequences," in *Australasian Joint Conference on Artificial Intelligence*, 2016.
- [12] A. Javaid, Q. Niyaz, W. Sun, and M. Alam, "A deep learning approach for network intrusion detection system," in *Proceedings of the 9th EAI International Conference on Bio-inspired Information and Communications Technologies (formerly BIONETICS)*, 2016.
- [13] T. A. Tang, L. Mhamdi, D. McLernon, S. A. R. Zaidi, and M. Ghogho, "Deep learning approach for network intrusion detection in software defined networking," in *2016 IEEE International Conference on Wireless Networks and Mobile Communications (WINCOM)*, IEEE, 2016.
- [14] S. M. Milajerdi, R. Gjomemo, B. Eshete, R. Sekar, and V. N. Venkatakrishnan, "Holmes - real-time apt detection through correlation of suspicious information flows.," in *IEEE Symposium on Security and Privacy (SP)*, 2019.
- [15] Q. Wang, W. U. Hassan, D. Li, *et al.*, "You are what you do: Hunting stealthy malware via data provenance analysis," in *Network and Distributed System Security Symposium (NDSS)*, Feb. 2020.
- [16] X. Han, T. Pasquier, A. Bates, J. Mickens, and M. Seltzer, "Unicorn: Runtime provenance-based detector for advanced persistent threats," in *Network and Distributed System Security Symposium (NDSS)*, Feb. 2020.
- [17] M. N. Hossain, S. Sheikhi, and R. Sekar, "Combating dependence explosion in forensic analysis using alternative tag propagation semantics," in *IEEE Symposium on Security and Privacy (SP)*, 2020.
- [18] X. Han, X. Yu, T. Pasquier, *et al.*, "Sigl: Securing software installations through deep graph learning," in *30th USENIX Security Symposium (SEC)*, 2021.
- [19] Z. Cheng, Q. Lv, J. Liang, *et al.*, "Kairos: Practical intrusion detection and investigation using whole-system provenance," in *IEEE Symposium on Security and Privacy (SP)*, 2024.
- [20] M. U. Rehman, H. Ahmadi, and W. U. Hassan, "Flash: A comprehensive approach to intrusion detection via provenance graph representation learning," in *IEEE Symposium on Security and Privacy (SP)*, 2024.
- [21] A. Goyal, G. Wang, and A. Bates, "R-caid: Embedding root cause analysis within provenance-based intrusion detection," in *IEEE Symposium on Security and Privacy (SP)*, 2024.
- [22] *What is xdr?* <https://tinyurl.com/mrymbmd5>, Accessed: April 6, 2023, 2022.
- [23] P. Firstbrook and C. Lawson, *Gartner reprint*, <https://www.gartner.com/doc/reprints?id=1-27NCOQL7&ct=211014&st=sb>, Accessed: April 1, 2023, 2022.
- [24] Vendor, *Endpoint detection and response (edr) solutions reviews 2022 | gartner peer insights*, <http://tinyurl.com/spturarb>, Accessed: April 1, 2023, 2022.

- [25] P. A. Team, *What is endpoint detection and response (edr)? - palo alto networks*, <http://tinyurl.com/3kt8btd2>, Accessed: April 1, 2023, 2022.
- [26] G. Karantzas and C. Patsakis, “An empirical assessment of endpoint security systems against advanced persistent threats attack vectors,” *CoRR*, 2021.
- [27] Z. Ying, D. Bourgeois, J. You, M. Zitnik, and J. Leskovec, “Gnnexplainer: Generating explanations for graph neural networks,” in *Neural Information Processing Systems (NeurIPS)*, 2019.
- [28] D. Luo, W. Cheng, D. Xu, *et al.*, “Parameterized explainer for graph neural network,” 2020.
- [29] H. Yuan, H. Yu, J. Wang, K. Li, and S. Ji, “On explainability of graph neural networks via subgraph explorations,” in *International Conference on Machine Learning (ICML)*, PMLR, 2021.
- [30] A. Warnecke, D. Arp, C. Wressnegger, and K. Rieck, “Don’t paint it black: White-box explanations for deep learning in computer security,” *CoRR*, 2019.
- [31] A. Warnecke, D. Arp, C. Wressnegger, and K. Rieck, “Evaluating explanation methods for deep learning in security,” in *2020 IEEE 7th European Symposium on Security and Privacy (EuroS&P)*, 2020.
- [32] T. Ganz, P. Rall, M. Härterich, and K. Rieck, “Hunting for truth: Analyzing explanation methods in learning-based vulnerability discovery,” in *2023 IEEE 8th European Symposium on Security and Privacy (EuroS&P)*, 2023.
- [33] A. K. Sood and S. Zeadally, “Drive-by download attacks: A comparative study,” *IT Professional*, 2016.
- [34] G. Phillips, *What is a drive-by download malware attack?* <http://tinyurl.com/yzbecvj5>, 2021.
- [35] *Trojan.win32.scar.ad*, <https://tinyurl.com/3sdj642z>, 2019.
- [36] *Mimikatz*, <http://tinyurl.com/3styvesw>, (Accessed on 01/21/2024), 2018.
- [37] G. O. Detecting and S. an APT41 Operation, *Mimikatz*, <http://tinyurl.com/mr4cdtyv>, (Accessed on 01/21/2024), 2023.
- [38] F. Pierazzi, F. Pendlebury, J. Cortellazzi, and L. Cavallaro, “Intriguing properties of adversarial ml attacks in the problem space,” in *IEEE Symposium on Security and Privacy (SP)*, 2020.
- [39] T. Ganz, M. Härterich, A. Warnecke, and K. Rieck, “Explaining graph neural networks for vulnerability discovery,” in *Proceedings of the 14th ACM Workshop on Artificial Intelligence and Security*, 2021.
- [40] J. Griffith, D. Kong, A. Caro, *et al.*, “Scalable transparency architecture for research collaboration (starc)-darpa transparent computing (tc) program,” Raytheon BBN Technologies Corp. Cambridge United States, Tech. Rep.
- [41] K. Mukherjee, J. Wiedemeier, T. Wang, *et al.*, “Evading provenance-based ml detectors with adversarial system actions,” in *32nd USENIX Security Symposium (SEC)*, 2023.
- [42] F. Barr-Smith, X. Ugarte-Pedrero, M. Graziano, R. Spolaor, and I. Martinovic, “Survivalism: Systematic analysis of windows malware living-off-the-land,” in *IEEE Symposium on Security and Privacy (SP)*, 2021.
- [43] S. T. King and P. M. Chen, “Backtracking intrusions,” in *USENIX Symposium on Operating Systems Design and Implementation (OSDI)*, 2003.
- [44] Y. Liu, M. Zhang, D. Li, *et al.*, “Towards a timely causality analysis for enterprise security,” in *Network and Distributed System Security Symposium (NDSS)*, Feb. 2018.
- [45] W. U. Hassan, S. Guo, D. Li, *et al.*, “Nodoze: Combatting threat alert fatigue with automated provenance triage,” in *Network and Distributed System Security Symposium (NDSS)*, Feb. 2019.
- [46] MITRE, *Mitre att&ck*®, <https://attack.mitre.org/>, Accessed: April 6, 2023.
- [47] *Virustotal*, <https://www.virustotal.com/>, Accessed: April 6, 2023, 2021.
- [48] *Metasploit*, <https://www.metasploit.com/>, (Accessed on 11/29/2021), 2021.
- [49] *Cobalt strike | adversary simulation and red team operations*, <https://www.cobaltstrike.com/>, 2023.
- [50] *Canvas*, <http://tinyurl.com/4bd7ann3>, 2023.
- [51] S. Forrest, S. Hofmeyr, A. Somayaji, and T. Longstaff, “A sense of self for unix processes,” in *IEEE Symposium on Security and Privacy (SP)*, 1996.
- [52] F. Yang, J. Xu, C. Xiong, Z. Li, and K. Zhang, “{Prographer}: An anomaly detection system based on provenance graph embedding,” in *32nd USENIX Security Symposium (SEC)*, 2023.
- [53] J. Zengy, X. Wang, J. Liu, *et al.*, “Shadewatcher: Recommendation-guided cyber threat analysis using system audit records,” in *IEEE Symposium on Security and Privacy (SP)*, 2022.
- [54] *Deep graph library: Easy deep learning on graphs*, <https://www.dgl.ai/>, (Accessed on 09/21/2021), 2022.

- [55] W. Guo, D. Mu, J. Xu, P. Su, G. Wang, and X. Xing, "Lemna: Explaining deep learning based security applications," in *ACM conference on Computer and Communications Security (CCS)*, Nov. 2018.
- [56] J. D. Herath, P. P. Wakodikar, P. Yang, and G. Yan, "Cfgexplainer: Explaining graph neural network-based malware classification from control flow graphs," in *2022 52nd Annual IEEE/IFIP International Conference on Dependable Systems and Networks (DSN)*, 2022.
- [57] M. Someya, Y. Otsubo, and A. Otsuka, "Fcgat: Interpretable malware classification method using function call graph and attention mechanism," in *Network and Distributed System Security Symposium (NDSS)*, vol. 1, Feb. 2023.
- [58] A. S. Jacobs, R. Beltiukov, W. Willinger, R. A. Ferreira, A. Gupta, and L. Z. Granville, "Ai/ml for network security: The emperor has no clothes," in *ACM Conference on Computer and Communications Security (CCS)*, Nov. 2022.
- [59] Canvas, <http://tinyurl.com/y4wrf74u>, 2023.
- [60] Canvas, <http://tinyurl.com/yaknev56>, 2023.
- [61] die.net, *Linux man page*, <https://linux.die.net/man/>, 2017.
- [62] M. Kosan, S. Verma, B. Armgaan, *et al.*, "Gnnx-bench: Unravelling the utility of perturbation-based gnn explainers through in-depth benchmarking," 2023.
- [63] H. Yuan, H. Yu, S. Gui, and S. Ji, "Explainability in graph neural networks: A taxonomic survey," *arXiv preprint arXiv:2012.15445*, 2020.
- [64] A. Goyal, X. Han, G. Wang, and A. Bates, "Sometimes, you aren't what you do: Mimicry attacks against provenance graph host intrusion detection systems," in *Network and Distributed System Security Symposium (NDSS)*, Feb. 2023.
- [65] ThreatIntelligence, *Mitre att&ck framework: All you ever wanted to know*, <http://tinyurl.com/5n6jt5pt>, 2023.
- [66] F. Barbero, F. Pendlebury, F. Pierazzi, and L. Cavallaro, "Transcending transcend: Revisiting malware classification in the presence of concept drift," in *IEEE Symposium on Security and Privacy (SP)*, 2022.
- [67] K. Paramonov, D. Shemetov, and J. Sharpnack, "Estimating graphlet statistics via lifting," in *Proceedings of the 25th ACM SIGKDD International Conference on Knowledge Discovery & Data Mining*, 2019.
- [68] M. Jha, C. Seshadhri, and A. Pinar, "Path sampling: A fast and provable method for estimating 4-vertex subgraph counts," in *Proceedings of the 24th international conference on world wide web*, 2015.
- [69] T. G. Kolda, A. Pinar, T. Plantenga, C. Seshadhri, and C. Task, "Counting triangles in massive graphs with mapreduce," *SIAM Journal on Scientific Computing*, 2014.
- [70] C. Seshadhri, A. Pinar, and T. G. Kolda, "Fast triangle counting through wedge sampling," in *Proceedings of the SIAM Conference on Data Mining*, 2013.
- [71] J. Ugander, L. Backstrom, and J. Kleinberg, "Subgraph frequencies: Mapping the empirical and extremal geography of large graph collections," in *Proceedings of the 22nd international conference on World Wide Web*, 2013.
- [72] M. ATT&CK®, *Exploitation for client execution*, <http://tinyurl.com/muhzctfb>, 2018.
- [73] M. ATT&CK®, *Data from local system*, <https://attack.mitre.org/techniques/T1005/>, 2017.
- [74] CrowdStrike, *Wannamine cryptomining: Harmless nuisance or disruptive threat?* <http://tinyurl.com/ycxvukjk>, 2018.
- [75] M. ATT&CK®, *Create or modify system process*, <https://attack.mitre.org/techniques/T1543/>, 2020.
- [76] K. P. Grammatikakis, I. Koufos, N. Kolokotronis, C. Vassilakis, and S. Shiaeles, "Understanding and mitigating banking trojans: From zeus to emotet," in *IEEE International Conference on Cyber Security and Resilience (CSR)*, 2021.
- [77] M. ATT&CK®, *System information discovery*, <https://attack.mitre.org/techniques/T1082/>, 2018.
- [78] K. Bareckas, *The mydoom worm: History, technical details, and defense*, <https://nordvpn.com/blog/mydoom-virus/>, 2022.
- [79] M. ATT&CK®, *Exfiltration*, <https://attack.mitre.org/tactics/TA0010/>, 2018.
- [80] M. Team, *Event tracing*, <http://tinyurl.com/4usynccm>, 2021.
- [81] Redhat, *The linux audit framework*, <https://github.com/linux-audit/>, 2017.
- [82] scikit Team, *Scikit*, <https://scikit-learn.org/stable/1>, 2021.
- [83] P. Veličković, G. Cucurull, A. Casanova, A. Romero, P. Lio, and Y. Bengio, "Graph attention networks," *arXiv preprint arXiv:1710.10903*, 2017.
- [84] W. Hamilton, Z. Ying, and J. Leskovec, "Inductive representation learning on large graphs," 2017.
- [85] A. Küchler, A. Mantovani, Y. Han, L. Bilge, and D. Balzarotti, "Does every second count? time-based evolution of malware behavior in sandboxes," in *Network and Distributed System Security Symposium (NDSS)*, Feb. 2021.

- [86] E. Avllazagaj, Z. Zhu, L. Bilge, D. Balzarotti, and T. Dumitras, “When malware changed its mind: An empirical study of variable program behaviors in the real world.,” in *30th USENIX Security Symposium (SEC)*, 2021.
- [87] *Cuckoo sandbox*, <https://tinyurl.com/33jdw93>, Accessed: April 6, 2023, 2019.
- [88] *Ntdll.dll*, <http://tinyurl.com/yc2z88px>, (Accessed on 01/21/2024), 2018.
- [89] *Bcryptprimitives.dll*, <http://tinyurl.com/yvpesvzt>, (Accessed on 01/21/2024), 2018.

A Appendix

A.1 Dataset Statistics

Anomaly Detection Dataset. The dataset statistics for the anomaly detection dataset is seen in Table 6. The Fileless Malware samples were downloaded from [47] and selected from recent studies, [42], [76], [85], [86]. The benign provenance graphs for the anomaly detection dataset were sourced from the DARPA dataset, which contained 5,695 benign graphs with an average of 669.81 vertices and 982.18 edges (Table 6); the Fileless Malware dataset, which contained 19,422 benign graphs with an average of 60.44 vertices and 54.15 edges; and the APT dataset, which contained 6,291 benign graphs with an average of 55.94 vertices and 83.29 edges. The corresponding anomaly graphs are sourced from the same datasets: The DARPA dataset contained 30 anomalous graphs with an average of 777.08 vertices and 1011.19 edges (Table 6); the Fileless Malware contained 1,043 anomalous graphs with an average of 63.72 vertices and 89.93 edges; and the APT dataset contained 2,928 anomalous graphs with an average of 58.38 vertices and 51.69 edges.

Classification Dataset. For program classification, we chose python from the Linux environment and powershell.exe and firefox.exe from the Windows environment for our classification evaluation. Python and powershell.exe are language interpreters with flexible behaviors. In the DARPA datasets, attackers leveraged firefox.exe in many scenarios to gain initial access. Therefore, we wanted to investigate how does firefox.exe behave under different benign workloads. The provenance graphs from Linux environment contained 190.62 vertices, 353.63 edges and 24925 graphs and Windows environment contained 295.31 vertices, 358.70 edges and 11710 graphs, on average (Table 7). From the program description in Table 5 it is clear that each type of program has distinctive behavior.

We chose five different classes of python programs as shown in Table 5. certbot is a ssl certificate management/update utility program, apt-xapian-index and unattended-upgrade are system programs that rebuild the

indexes and updates the linux distribution without user interface, respectively. cuckoo [87] is a sandbox utility that runs programs inside a sandbox and capture the system level interactions. certbot and cuckoo will have several outgoing network connections, but certbot’s outbound network connection will have higher number of connection to external IPs as compared to cuckoo. apt-xapian-index and unattended-upgrade, even though they are system utilities, behave differently in the sense that unattended-upgrade reads from many shared files such as .lock files and writes to specific .log files, but apt-xapian-index reads a lot of shared .so and .db files; apt-xapian-index also creates children who read from the same file .db files, so there is information transfer.

The classes for powershell.exe include four different kinds of execution policy, unrestricted, allsigned, restricted, bypass, and two execution configuration noLogo, and noInputformat. The class unrestricted permits the execution of all PowerShell scripts, including those downloaded from the internet *i.e.*, for application updates. The allsigned class enhances security by requiring that all scripts and configuration files be signed by a trusted publisher before execution. The default policy, restricted, offers a high level of security by preventing the execution of any scripts. In contrast, bypass allows scripts to run without any restrictions, which is commonly employed for troubleshooting purposes. The noLogo class is used to start PowerShell without displaying the logo and to disable prompts, scripts, and interactive input, making it suitable for automation tasks. Finally, noInputformat specifies that PowerShell no input is expected, a mode to execute scripts in a non-interactive environment without any external input.

The classes for firefox.exe encompass: moz_log, osint, jsInit, win32kLockedDown, and file. These classes reflect various Firefox execution modes and debugging options. The moz_log class is used to enable detailed logging in Firefox. The osint class indicates that Firefox is being launched for an external URL or file, typically seen in scenarios where the browser is invoked by other applications or operating system components (*e.g.*, discord.exe or slack.exe). The jsInit is a technical flag related to JavaScript engine initialization for internal debugging. The win32kLockedDown class is associated with security features, where Firefox operates with restricted access to certain system calls, typically used to mitigate risks of kernel vulnerabilities. The file class captures the direct opening of local files.

A.2 Ablation Study (using GraphSAGE)

The ablation study utilizing the GraphSAGE network revealed patterns consistent with those observed in the GAT network study (§5.4), particularly regarding the impact of certain shape groups on PROVEXPLAINER. Notably, the *Square* and *Kite* shapes were distinctively influential for datasets like

Table 5: Datasets used for classification: python(linux), powershell.exe and, firefox.exe.

| Program | Categories | Description |
|----------------|-------------------------|---|
| Linux | | |
| python | cerbot | Program is a ssl certificate management/update utility program. |
| | update-apt-xapian-index | System programs that rebuild the indexes index to sorts of extra information, such as Debtags tags, and package ratings. |
| | unattended-upgrade | System program that updates the linux distribution without user interface |
| | decompile3 | Custom python decompilation program that recovers the source code of python programs from their compiled bytecode instructions. |
| | cuckoo | Sandbox utility that lets the user run programs inside a sandbox and capture the system level interactions. |
| Windows | | |
| powershell.exe | unrestricted | Executes a unrestricted hidden script to disable unused SMBv1 protocol features. |
| | allSigned | Sets output encoding to UTF-8 and starts opening a file stream for only signed scripts. |
| | restricted | Executes a simple display command under a restricted policy, allowing no scripts. |
| | bypass | Bypasses the execution policy in PowerShell. |
| | noLogo | Runs PowerShell bypassing the execution policy, without the PowerShell logo, user profile, and interactively. |
| | noInputFormat | Runs PowerShell in a non-interactive mode, with input format set to none and output format set to text. |
| firefox.exe | moz_log | Enables detailed logging and runs a background tasks (e.g., updates). |
| | osint | Opens a specific URL, invoked by an external application (e.g., discord). |
| | jsInit | Starts a internal content rendering process with detailed parameters for communication and preferences. |
| | win32LockedDown | Initializes a secured sandbox environment for content in Firefox with specific build details. |
| | file | Opens a local HTML or PDF file. |

Table 6: APT and Fileless Malware graph statistics.

| Applications | # of Benign Graphs | # of Anomaly Graphs | Avg # of Benign Nodes / Edges | Avg # of Anomaly Nodes / Edges |
|----------------------------|--------------------|---------------------|-------------------------------|--------------------------------|
| DARPA APT Dataset [40] | | | | |
| Trace | 1883 | 8 | 735.35 / 957.56 | 836.15 / 946.75 |
| Theia | 2858 | 9 | 559.47 / 979.59 | 913.91 / 987.31 |
| FiveDirections | 954 | 13 | 906.22 / 971.91 | 959.43 / 973.63 |
| Average | 1898.33 | 10.00 | 669.81 / 982.18 | 777.08 / 1011.19 |
| APT Dataset from [41] | | | | |
| Enterprise | 3079 | 1836 | 90.22 / 85.13 | 73.73 / 76.88 |
| Supply-Chain | 3212 | 1092 | 65.02 / 40.77 | 61.09 / 54.33 |
| Average | 3145.50 | 1464.00 | 55.94 / 83.29 | 58.38 / 51.69 |
| Fileless Malware from [42] | | | | |
| explorer.exe | 399 | 40 | 66.18 / 59.94 | 44.10 / 56.45 |
| wmic.exe | 876 | 11 | 88.56 / 81.58 | 87.36 / 101.54 |
| reg.exe | 309 | 116 | 60.18 / 52.93 | 78.91 / 131.87 |
| sc.exe | 621 | 7 | 44.08 / 37.49 | 38.42 / 52.28 |
| python.exe | 15585 | 426 | 89.95 / 83.15 | 57.98 / 79.33 |
| svchost.exe | 1632 | 443 | 52.42 / 46.42 | 51.97 / 81.31 |
| Average | 2667.00 | 90.84 | 60.44 / 54.15 | 63.72 / 89.93 |

Fileless Malware. These shapes effectively encapsulate malware replication and deployment processes. Additionally, the *Square* and *Kite* shapes demonstrated notable performance in the APT dataset from [41]. This effectiveness is attributed to their ability to capture shared dependencies, a vital element in the *initial access* and *establishing a foothold* stages of an attacker’s APT campaign—a finding consistent with their performance in the GAT network analysis.

In the context of the DARPA APT dataset, the *exploding shapes* assumed significant importance. This dataset, characterized by numerous long-range dependencies associated with malware, finds an effective representation through the *exploding shapes*. These shapes are particularly adept at capturing

Table 7: Classification dataset graph statistics.

| Program | Categories | Avg Nodes / Edges | Graphs |
|----------------|-------------------------|------------------------|-----------------|
| Linux | | | |
| python | certbot | 74.85 / 149.94 | 4955 |
| | update-apt-xapian-index | 169.78 / 302.37 | 4922 |
| | unattended-upgrade | 742.24 / 312.56 | 4966 |
| | decompile3 | 90.67 / 169.61 | 5010 |
| | cuckoo | 305.26 / 403.99 | 5072 |
| Average | | 190.62 / 353.63 | 24925.00 |
| Windows | | | |
| powershell.exe | unrestricted | 71.20 / 172.10 | 2704 |
| | allsigned | 815.50 / 917.10 | 1123 |
| | restricted | 100.00 / 129.60 | 1002 |
| | bypass | 639.40 / 713.40 | 1074 |
| | noLogo | 691.40 / 743.70 | 780 |
| | noInputFormat | 195.00 / 283.70 | 614 |
| firefox.exe | moz_log | 249.80 / 340.40 | 918 |
| | osint | 95.50 / 115.60 | 323 |
| | jsInit | 144.50 / 183.10 | 14051 |
| | win32LockedDown | 102.30 / 124.20 | 741 |
| | file | 143.80 / 222.80 | 91 |
| Average | | 295.31 / 358.70 | 11710.50 |

scenarios that represent the later stages of an APT campaign, such as *deepen access* and *lateral movement*. These stages are typically marked by malware activities involving reading several system dependencies or probing system files so that the malware can replicate and spread.

A.3 PROVEXPLAINER vs. SOTA Explainers (using GraphSAGE)

As mentioned previously §5.1, we use precision and recall to compare the explanation quality of PROVEXPLAINER and

Table 8: WMA F1 of surrogate DTs approximating a GraphSAGE model across different feature subsets. The best feature subsets are bolded.

| Dataset | Number of nodes and edges | Security Domain Features §4.1 | | | | | All Security Domain Features |
|----------------------------|---------------------------|-------------------------------|---------------------|---------------------|-----------------------|--------------------------|------------------------------|
| | | Triangles | Squares and Kites | Exploding Shapes | Cascade and Jellyfish | Internal vs External IPs | |
| DARPA APT Dataset | | | | | | | |
| FiveDirections | 0.58 (-0.32) | 0.74 (-0.16) | 0.88 (-0.02) | 0.88 (-0.02) | 0.71 (-0.19) | 0.75 (-0.15) | 0.90 |
| Trace | 0.61 (-0.31) | 0.73 (-0.19) | 0.81 (-0.11) | 0.86 (-0.06) | 0.86 (-0.06) | 0.81 (-0.11) | 0.92 |
| Theia | 0.58 (-0.32) | 0.79 (-0.11) | 0.81 (-0.09) | 0.87 (-0.03) | 0.84 (-0.06) | 0.82 (-0.08) | 0.90 |
| Average | 0.59 (-0.32) | 0.75 (-0.15) | 0.83 (-0.07) | 0.87 (-0.04) | 0.80 (-0.10) | 0.79 (-0.11) | 0.91 |
| APT Dataset from [41] | | | | | | | |
| Enterprise | 0.72 (-0.18) | 0.78 (-0.12) | 0.70 (-0.20) | 0.63 (-0.27) | 0.63 (-0.27) | 0.67 (-0.23) | 0.90 |
| Supply-Chain | 0.75 (-0.16) | 0.76 (-0.15) | 0.87 (-0.04) | 0.87 (-0.04) | 0.84 (-0.07) | 0.87 (-0.04) | 0.91 |
| Average | 0.73 (-0.17) | 0.77 (-0.14) | 0.78 (-0.12) | 0.75 (-0.16) | 0.73 (-0.17) | 0.77 (-0.14) | 0.91 |
| Fileless Malware from [42] | | | | | | | |
| explorer.exe | 0.57 (-0.10) | 0.66 (-0.01) | 0.67 (0.00) | 0.65 (-0.02) | 0.63 (-0.04) | 0.54 (-0.13) | 0.67 |
| wmic.exe | 0.49 (-0.40) | 0.85 (-0.04) | 0.88 (-0.01) | 0.81 (-0.08) | 0.82 (-0.07) | 0.87 (-0.02) | 0.89 |
| reg.exe | 0.87 (-0.06) | 0.37 (-0.56) | 0.93 (0.00) | 0.88 (-0.05) | 0.92 (-0.01) | 0.49 (-0.44) | 0.93 |
| sc.exe | 0.49 (-0.44) | 0.84 (-0.09) | 0.91 (-0.02) | 0.87 (-0.06) | 0.91 (-0.02) | 0.83 (-0.10) | 0.93 |
| python.exe | 0.71 (-0.04) | 0.68 (-0.07) | 0.74 (-0.01) | 0.74 (-0.01) | 0.72 (-0.03) | 0.67 (-0.08) | 0.75 |
| svchost.exe | 0.74 (-0.07) | 0.81 (0.00) | 0.75 (-0.06) | 0.78 (-0.03) | 0.75 (-0.06) | 0.78 (-0.03) | 0.81 |
| Average | 0.65 (-0.19) | 0.70 (-0.13) | 0.81 (-0.02) | 0.79 (-0.04) | 0.79 (-0.04) | 0.70 (-0.13) | 0.83 |
| Program Classification | | | | | | | |
| python | 0.53 (-0.18) | 0.61 (-0.10) | 0.69 (-0.02) | 0.65 (-0.06) | 0.70 (-0.01) | 0.67 (-0.04) | 0.71 |
| powershell.exe | 0.63 (-0.34) | 0.84 (-0.13) | 0.74 (-0.23) | 0.82 (-0.15) | 0.69 (-0.28) | 0.91 (-0.06) | 0.97 |
| firefox.exe | 0.37 (-0.33) | 0.41 (-0.29) | 0.45 (-0.25) | 0.51 (-0.19) | 0.41 (-0.29) | 0.64 (-0.06) | 0.70 |
| Average | 0.53 (-0.18) | 0.61 (-0.10) | 0.69 (-0.02) | 0.65 (-0.06) | 0.70 (-0.01) | 0.67 (-0.04) | 0.71 |

Precision and Recall of Different Graph Neural Network Explainers

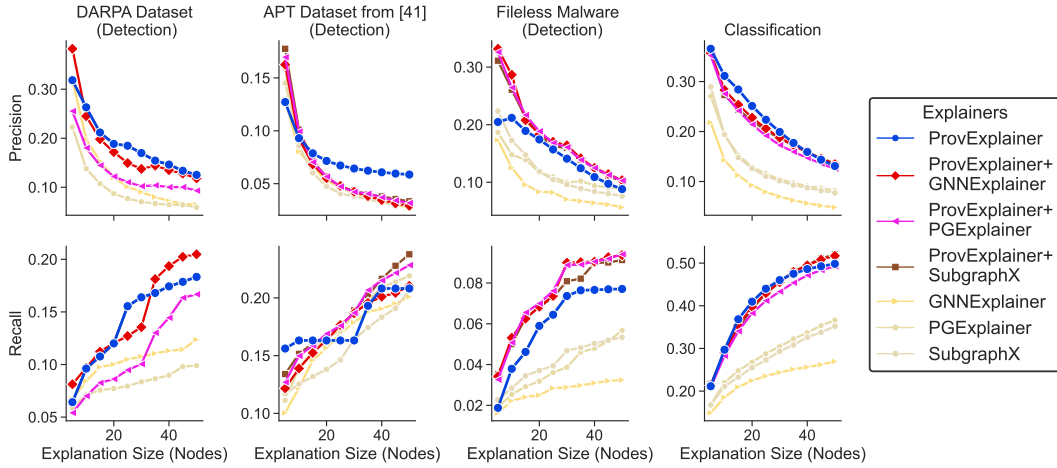


Figure 8: Effectiveness of graph model explainers at identifying documented entities (§5.1), measured using precision and recall as more nodes are included in the explanation. PROVEXPLAINER outperforms SOTA explainers on anomaly detection tasks and remains competitive in classification tasks.

SOTA GNN explainer (GNNEExplainer, PGExplainer, and SubgraphX). Similar to GAT based results, PROVEXPLAINER deliver the best performance across the datasets. The complexity (*i.e.*, size and resource interaction) of the provenance graphs play a major role in determining which explainers would be effective for a particular dataset. For smaller provenance graphs like APT graphs from [41] PGExplainer performs the second best but for DARPA APT graphs which are known to be complex or noisy GNNEExplainer performs

the second best. Fileless Malware dataset’s malware graph composure is different as compared to APT attacks due to the attack campaigns. So, SubgraphX performed better than both GNNEExplainer and PGExplainer. SubgraphX showed its specialization in identifying the distinctive malicious subgraphs which when removed changes the model prediction. However, this specialization also lead to limitations in other scenarios, particularly where the malware is making succinct changes in the system to avoid detection, *e.g.*, APT scenarios.

An interesting trend is that while PROVEXPLAINER performed the best in both the DARPA and APT datasets, the second-best explainer for DARPA is GNNExplainer, while for the APT dataset it is PGExplainer. GNNExplainer tries to identify potentially disjoint substructures that maximize mutual information, but PGExplainer generates a probabilistic global model to explain the predictions. This interesting trend showcases that while GNNExplainer is more suitable when the focus is on understanding specific decisions made by the GNN, and PGExplainer is better suited for scenarios where a global explanation across the dataset is necessary. Since, the two explainers perform at different capacity for the datasets, it gives insight regarding the composition of the dataset *i.e.*, is it easier to create global explanations that are consistent throughout the dataset or is it more apt to create local explanations. For the DARPA datasets it is hard to create generalized explanations since the DARPA dataset consists of different APT scenario that are executed using different payload and attack tactics. But, for the APT dataset which majorly consists of only two different APT scenarios (*e.g.*, Enterprise and Supply-Chain APT), it is easier to create global explanations, so PGExplainer was able to create global explanations that are consistent across datasets.

A.4 Case Studies: In-Depth Analysis

FiveDirections: Browser Extension. In the context of the described attack, where the drakon malware exploits the firefox.exe browser through a rogue extension (pass_mgr) the Jellyfish shape is created. Multiple instances of the malware process are created, each reading from the malicious files: pass_mgr.exe and passwordfile.dat. Additionally, they access essential dictionary files (en-US.aff) and cryptographic libraries (bcryptprimitives.dll) to maintain operational consistency, allowing them to conduct their malicious activities efficiently. The Exploding Square shape captures the data extraction behavior through sensitive file accesses. These malware access sensitive information and system configuration files like WindowsShell.Manifest, shell32.dll, cryptbase.dll, and wintrust.dll, along with initial malware files (addons, tzres.dll, userenv.dll).

GNNExplainer effectively identifies the malware template file present in C:\ProgramFiles\MozillaFirefox\add-on\pass_mgr.exe and the initial malware pass_mgr.exe. PGExplainer recognized the structures common across all attack graphs, particularly identifying file access of system libraries needed for malware operation C:*\System32\driver, C:*\Windows\SysWOW64 and C:*\AppData\Local\Temp. SubgraphX performed at the same capacity as PGExplainer as it identified a different the structure of malware executing its payload from C:*\Desktop*\add-on, reading sensitive files from C:*\ProgramFiles\MozillaFirefox*, and extracting them through C:*\admin\AppData*. This is partly due

to its foundation on Monte Carlo Tree Search (MCTS), incorporating nondeterministic exploitation and exploration stages. In the absence of attribute information in the GNN, the exploitation stage lacks guidance. But, when SubgraphX correctly identifies a substructure for exploitation, the exploration stage of MCTS proves effective.

FiveDirections: Copykatz. The Dropper Triangle starts its kill chain stage of initial access [72] by reading shared dynamic-link libraries (DLLs); notable mentions are ntdll.dll and bcryptprimitives.dll. It then writes and executes a malware masquerading as firefox.exe which contains the Mimikatz and Copykatz modules. ntdll.dll [88] includes multiple kernel-mode functions which enables the “Windows Application Programming Interface (API)” and bcryptprimitives.dll [89] contain functions implementing cryptographic primitives, which are essential for Mimikatz [36] and Copykatz to function.

The firefox.exe malware write its payload into temporary files, such as virtuous and tropical. Subsequently, another malicious instance of the firefox.exe malware initiates a domino effect by creating a chain of processes by executing the malware template. This dependency correlation between the malware and its parent is characterized by functional inheritance, where the children require the same system library files as the parent to function correctly. The DLLs involved are read from ProgramFiles and System32.

GNNExplainer and PGExplainer correctly identified the data extraction stage where four malicious firefox.exe processes make C2 connections to the external IPs (202.179.137.58 and 217.160.205.44). firefox.exe was invoked by malware masquerading as runtimebroker.exe, so if GNNExplainer masks out the process creation edge of the children firefox.exe, that would lead to a graph cut with two separate graphs, leading to a change in the prediction. SubgraphX also highlighted similar firefox.exe processes that are created by the first runtimebroker.exe, but instead of making external C2 connection it created another firefox.exe process for rendering content from localhost (127.0.0.1).

Trace: Phishing E-mail. The Probe Triangle captured the staging behavior of the Trojan. The Trojan was downloaded from www.nasa.ng, executed and replicated itself within the system. Specifically, the malware named nasa.ng is placed in /home/admin/.mozilla/firefox/ and /usr/local/firefox-54.0.1/obj-x86_64-pc-linux-gnu/. The Trojan created new malware with benign names such as firefox to effectively evade detectors, to replicate unhindered and overloaded the system with malicious processes. After the malware successfully staged, the malware masquerading as /bin/sh to read the malicious script staged in (/etc/update-motd.d/00-header/) and executed it to create multiple copies of itself. The malware reads various system configuration files present in /etc/protocols/, /etc/lsb-release/, and /etc/hosts.deny/. Reading sensitive

system configuration files are essential to build the system profile. The *Jellyfish* shape captured the dependency correlation of the malwares being created that inherited similar configuration.

Ultimately, the malware completes its target of reading sensitive system files from `/etc/fonts/conf.d/`, `/usr/lib/x86_64-linux-gnu/`, and `/usr/share/X11/local/`. These activities are aimed at gathering system information to create a profile of the company and the devices in use. The attacker wants to create a profile of the victim environment to ensure their malware can effectively leverage system libraries to complete their objective. There is an overlap in the files (present in `\etc\hosts` and `/usr/lib/x86_64-linux-gnu/*`) involved in the *Probe Triangle* and *Jelly-*

fish operations because the malware replicates itself probing and inheriting the functional dependencies of its parent.

GNNExplainer was able to correctly capture the staging behavior where the malware from `nasa.ng` read shared library (`/usr/lib/x86_64-linux-gnu/*.so.*`) and cache file (`/usr/share/applications/mimeinfo.cache`, `/usr/lib/x86_64-linux-gnu*/loaders.cache`). PG-Explainer incorrectly indicated benign substructures, but SubgraphX correctly captured the inheritance behavior of `firefox.exe` executing multiple times with the argument file `http://www.nasa.ng/`, to create the malware clones from the template. SOTA explainers missed the malware's ultimate goal of reading sensitive files, which was only captured by PROVEXPLAINER.